

# A new optimization approach for the use of hybrid renewable systems in the search of the zero net energy consumption in water irrigation systems

Angel V. Mercedes García<sup>a</sup>, Francisco Javier Sánchez-Romero<sup>b</sup>,  
P. Amparo López-Jiménez<sup>a</sup>, Modesto Pérez-Sánchez<sup>a,\*</sup>

<sup>a</sup> Hydraulic Engineering and Environment Department, Universitat Politècnica de València, Valencia, 46022, Spain

<sup>b</sup> Rural and Agrifood Engineering Department, Universitat Politècnica de València, Valencia, 46022, Spain

## ARTICLE INFO

### Article history:

Received 29 November 2021

Received in revised form

31 May 2022

Accepted 11 June 2022

Available online 22 June 2022

### Keywords:

Hybrid renewable systems (HRS)

Simulated annealing

Irrigations networks

Solar pumped

Microhydropowers

Sustainable management

## ABSTRACT

The search of the sustainability in the water system and the improvement of the different targets, which are included in the different sustainable development goals. It implies the water managers must define new strategies, which define the establishment of new investment and making-decision in this alignment. The new proposed approach proposes the use of hybrid renewable systems, which are optimized by two simulated annealing procedures included inside of the methodology. It is applied in a real irrigation network where there are pump stations. The methodology chooses the best location of the microhydropowers systems and the selection of the best machine between a database of 674 pump working as turbines defining the minimum area of photovoltaic systems to be feasible the hybrid renewable system by a techno-economical analysis. The applied optimization procedure reached an annual average self-consumption energy value above 0.9, showing an annual positive energy balance of 283 MWh, using renewable energies and they could be sold to the grid. The environmental analysis shows both an annual reduction of 2838 tones of CO<sub>2</sub> emissions and 553 MWh generated using non-renewable energies.

© 2022 Published by Elsevier Ltd.

## 1. Introduction

Energy needs water, and water needs energy, this relationship is an interdependence on which the scientific world has been focusing its attention in recent decades [1]. Numerous studies seek to determine the sustainability condition of water distribution networks. One of the most famous of these is the United Nations by Sustainable Development Goals (SDGs), which aim to achieve optimal goods and services for all human beings [2]. Water service is affected by the demand for this service. The increase in demand due to population growth has created the need to look for new energy sources to supply the equipment in a more sustainable manner [3]. Currently, the improvement of the living standards and the increase of sustainable water management strategies [4]. The search for efficiency improvement caused different international

and national programs, which are focusing on developing strategies to enhance the adaptive features of water governance [5].

Water management cannot leave out the irrigation use. Agriculture consumes 70% of the fresh water withdrawn per year approximately. It implies the optimal use of water resources, as well as the improvement of the efficiency in its captation and distribution, will be the main challenges worldwide [6]. This challenge was established by the different countries, developing policies, which searched the improvement of irrigation schemes, the saving water and its adaptability, mainly in developing countries [7]. Europe defined different directive frameworks, which were focused on the improvement of irrigation efficiency since 2000 [8]. In this line, the Spanish government carried out an intense irrigation modernization process between 2002 and 2015. The main aim of this modernization was to achieve significant water savings, increase flexibility and guarantee the supply [9].

These improvements joined to new challenges, which search the use the renewable energies to reduce carbon emissions and to increase the sustainability of the different systems obligate to

\* Corresponding author.

E-mail addresses: [fcosanro@agf.upv.es](mailto:fcosanro@agf.upv.es) (F.J. Sánchez-Romero), [mopesan1@upv.es](mailto:mopesan1@upv.es) (M. Pérez-Sánchez).

consider new management analyzing the nexus water-energy. European Union fixed targets on 20% of the consumed energy should be obtained by renewable technologies [10]. It implies the agricultural area, which has high solar radiation values, the photovoltaic technology represents a clean strategy to generate energy to supply the different consumption in the water distribution systems [11].

The use of photovoltaic panels (PVP) as a source of energy for pumping stations is one of the alternatives that is gaining more fame because it is one of the most promising applications that can be assigned to this technology [12]. Places that are located in areas remote from the urban center, non-electrified and/or isolated are opting for the installation of this alternative because it facilitates the water supply in these areas, defining the following functions: (i) to integrate the rural communities [13], (ii) to constitute a potential option to draw down water in the remote locations [14], (iii) to improve the sustainable development of these communities towards zero-net energy consumption [15].

The incorporation of a pumping system based on the use of solar energy can generate better control of the system and also minimize the use of water losses in the distribution network [16]. In these lines, different approaches were defined to take advantage of the used surface to install a photovoltaic system both ground (called a ground-mounted photovoltaic panel, GPV) and floating in the free surface of the reservoirs (called floating photovoltaic panel, FPV) [17]. In any used system, the variation in the intensity of solar radiation causes the energy production does not remain constant throughout the day [18]. Therefore, storage is necessary using a battery bank, especially for pumping systems that aim to meet the demand regularly, guarantee the service at times when the production of electricity is lower or even zero and avoid the lack of power [19]. Studies even indicate the inclusion of energy storage systems [20]. Their oversizing can preserve and reduce the pump engine from energy production reductions due to climatic conditions [21].

These green supplies of energy were considered by different researchers. As an example of some of them [22], proposed a perturb/observed algorithm, which improved the overall system efficiency. An energy management control strategy was optimized by Ref. [23]. The strategy proposed an optimized control to maximize the effectiveness of the pump storage hydroelectric double effect system in the irrigation and electrical power restitution. It operated under the condition of constant flow since it will be focused on storage. The challenge was focused on improving the return rate compared to the traditional PV system [23]. increased return rate above 30% compared with the traditional PV system [24]. developed a review of the different variables of the objective functions as well as the different optimization techniques used by the different solutions of the problem by multi-objective optimization approaches as linear programming strategies. The analysis of this research showed there were few researchers, which considered the use of hybrid renewable energies applied to hourly demanded water systems [25]. proposed a stochastic strategy to minimize the operation cost in a daily pumped-storage unit and irrigation system. It was based on forecasted wind power, microgrid load demand and water needed for irrigation in a market environment, decreasing the annual operation cost above 110,000 € [26]. proposed a modified isotropic model, which defined the best strategy to pump water to an irrigation pond, minimizing the water consumption. Besides [26], showed different review values of the literature according to average mitigation cost of reduction of CO<sub>2</sub> (153€/tonneCO<sub>2</sub>), the average value of net present values, although the energy return on investment depended on the PV generator dimension. The energy payback time was between 1.94 and 5.25 years while the carbon payback time varied between 4.62 and 9.38

years [27]. established a review of the electric power generation with the help of solar panel/thermoelectric generator/Rakine cycle based technology applied to irrigation systems. As in previous cases, the irrigation pump operated to the reservoir and it implied the optimization was established to control the volume of the reservoir. The development of strategies, which were focused on optimized the hybrid renewable systems did not consider the reservoir or controlled demanded is reduced. Therefore, the analysis of optimization strategies is necessary when the free demand of the users, the system is pumped partial or totally and the farmed area can vary over time.

[28] established the analysis of PV systems combined with desalination shown Levelized Cost Of Energy (LCOE) equal to 43€/MWh [29]. developed a comparison between parabolic trough pump, concentrating dish pump and photovoltaic pump in Sudan. They reached LCOE values of 30, 53.36 and 68.18 €/MWh, respectively [30]. proposed a genetic algorithm model to find the optimal photovoltaic panel water system size, considering the maximum profit as an objective function, showing an improvement in the annual profit of 18%. A multiobjective optimization procedure was established by Ref. [31]. The research defined the most efficient combination of hydrants and subunits to be opened simultaneously in an irrigation pumped network. The objective function was to minimize the number of solar photovoltaic panels and the energy consumption required to drive pumping devices directly connected to solar panels, reaching a minimum daily energy consumption of 429 kWh without showing the economic values [29]. proposed a two-stage optimization strategy, which was carried out in an intelligent microgrid system considering the load management and the energy storage enhancement. The proposal increased the irrigation efficiency above 10% [32]. developed a hybrid optimized system using HOMER, which considered photovoltaic/diesel system simulated to change the diesel generators required for water pumping systems. The optimization was focused on minimizing the LCOE value, reaching operation management of 60% using renewable energies. A hybrid optimization by genetic algorithms software was proposed by Ref. [33], which showed LCOE values, which oscillated between 13 and 108 €/MWh as a function of the hybrid scenario.

In these conditions, the support of the system can also be carried out using variable frequency drivers, which achieves higher efficiency points in the work of the pumping equipment and, at the same time, increases the useful life of the pumping equipment [34]. The design of the PV for pumping systems must be able to guarantee the optimum operating point to improve the efficiency of the system [35]. Studies indicate that the use of photovoltaic panels for pumping systems can reduce greenhouse gas emissions by an important proportion [36]. In this line, the improvement of water management is introducing the use of a micro-hydropower system to increase the energy efficiency and reduce the energy, which is dissipated in pressure reduction valves [37]. The installations of these systems enable energy generation, which can be used for self-consumption if the recovery systems are near the consumption points [38]. These hydraulic recovery systems were studied for different researchers who established the best operation mode [39], regulation strategies [40], optimization strategies for the locations in water supply networks [41] and used hybrid with PV systems [42].

Mixing PV systems and microhydropower systems [43], developed a comparative analysis between a hybrid pump-as-turbine/solar pilot system (PAT-PV) and a traditional diesel generator. The research analysed the economic and environmental evaluation but it did not show any optimization procedure. The payback period of the analyses was eight years and the energy demand was only 2% of the potential generation of the hybrid system. The CO<sub>2</sub> emission

was  $2.6 \text{ gCO}_{2\text{eq}} \cdot \text{kWh}^{-1}$ , which was 30 times lower than the traditional non-renewable system. When the hybrid system (PAT-PV system) was compared with PV system only, the carbon emission varied from 57.6 to  $92 \text{ gCO}_{2\text{eq}} \cdot \text{kWh}^{-1}$ , respectively.

The alignment of these technologies in water management is necessary because the energy use in the water sector is growing, and all the quality requirements need to adapt to climate change while the reduction of greenhouse gases emissions [44]. The reach of the different targets of the sustainable development goals (SDG), which improve the quality of the environment is crucial, including the reduction of carbon dioxide and other gases that promote climate change, which generates the implementation of proposals to control emissions [45]. In the water sector, the cost of water is largely due to the operation and efficiency of distribution systems [46]. Several analyses show how implementing system operation policies can result in improved sustainability of water distribution networks, as well as improvement in the management of the energy required [44]. In this line, the proposed sustainable indicators are necessary to evaluate the water systems and the water management have tools for evaluating their making decisions as well as knowing their evolution over time.

This research proposes a methodology to integrate the use of hybrid systems, particularly GPV, FPV and micro hydropower systems in irrigation water systems, which have pumped areas in their irrigation area. The research proposes an optimization strategy, which evaluates the energy needs and it establishes the best location of the micro hydropower system, defining the minimum feasible area of GPV and FPV for reaching the zero-net consumption of non-renewable energies. The strategy considers economic indexes for the optimization procedure and it develops the evaluation of the sustainable indicators to evaluate the water operation. The optimization procedure is applied to irrigation systems, which operate considering flow on demand. It is a real novelty since the analysis of energy needs and analysis of the possibility to generate renewable energy to be self-consumption is not already developed. The operation scheme is defined in Fig. 1.

The research proposes the optimization of the FPV and GPV as a function of the farmed area, the recovered energy using micro-hydropower system integrated into a gravity system and a flow on-demand in the water system. This generated energy will be consumed at the consumption point, particularly, at different pumping stations. The energy excess could be stored using

batteries or they would be sold to the grid. The methodology minimizes the need to purchase energy for the grid when the hybrid system is not able to supply the energy demand. The novel is focused on the capacity to work with irrigation system, which operates on-demand both gravity and pumped systems and this management is discretized hourly. The manuscript is organized in a literature background, which is described in this section. The second section develops the proposed methodology. The third section is divided into five sections in which (i) the case study is described; (ii) the results of the optimization procedure of the hydraulic recovery system are shown; (iii) the analysis of the influence of farmed area is exposed according to hybrid system optimization; (iv) the energy balance and renewable analysis is exposed; and (v) a discussion of the optimum solutions. The fourth section contains the conclusions of the research.

## 2. Material and methods

The proposed methodology is divided into five different blocks (Fig. 2), which consider the hydraulic operation of the system (Block A), the photovoltaic generation (Block B), Economic Analysis (Block C), Environmental analysis (Block D) and the Techno-Feasibility model (Block E). The last block integrated all previous block systems optimized the making-decision considering the previous blocks according to Fig. 2, which shows the relationship between blocks. Block A contains two simulated annealing procedures to develop the optimization procedure related to the hydraulic network while Block B establishes the photovoltaic analysis to be implemented in Block E, which analysis the different renewable systems as a function of the flow on-demand, farmed area as well as economic conditions.

This first block is defined by four different steps: network model (A.1), energy balance (A.2), pumped analysis (A.3) and recovery analysis (A.4). The first step has the main goal to define the flow and pressure in each point over time. In this case, a model is developed using EPANET [47]. The patterns are defined in each irrigation point considering the irrigation needs. The network considers the different reservoirs, which supply different irrigation areas. These reservoirs can supply the demand at each moment, considering the variable irrigation area as a function of the scenario as well as the evapotranspiration.

The developed model is used in the second step (A.2) to develop

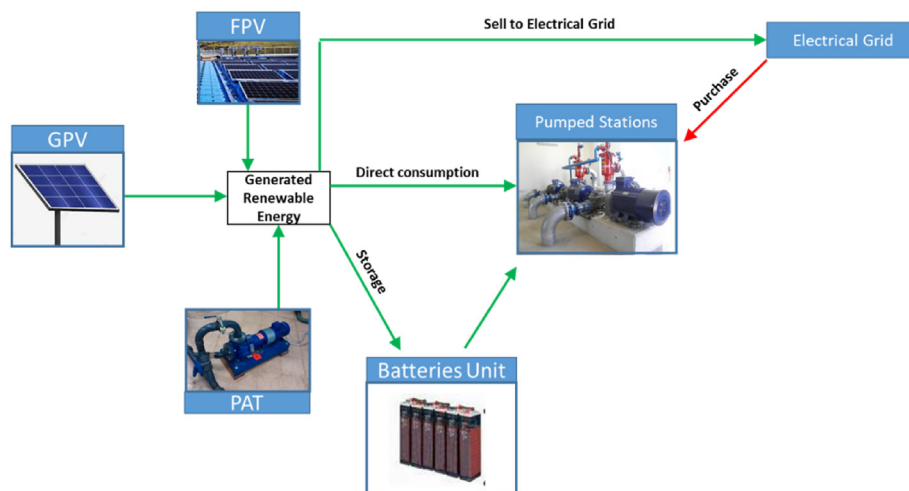


Fig. 1. Overall efficiency Scheme.

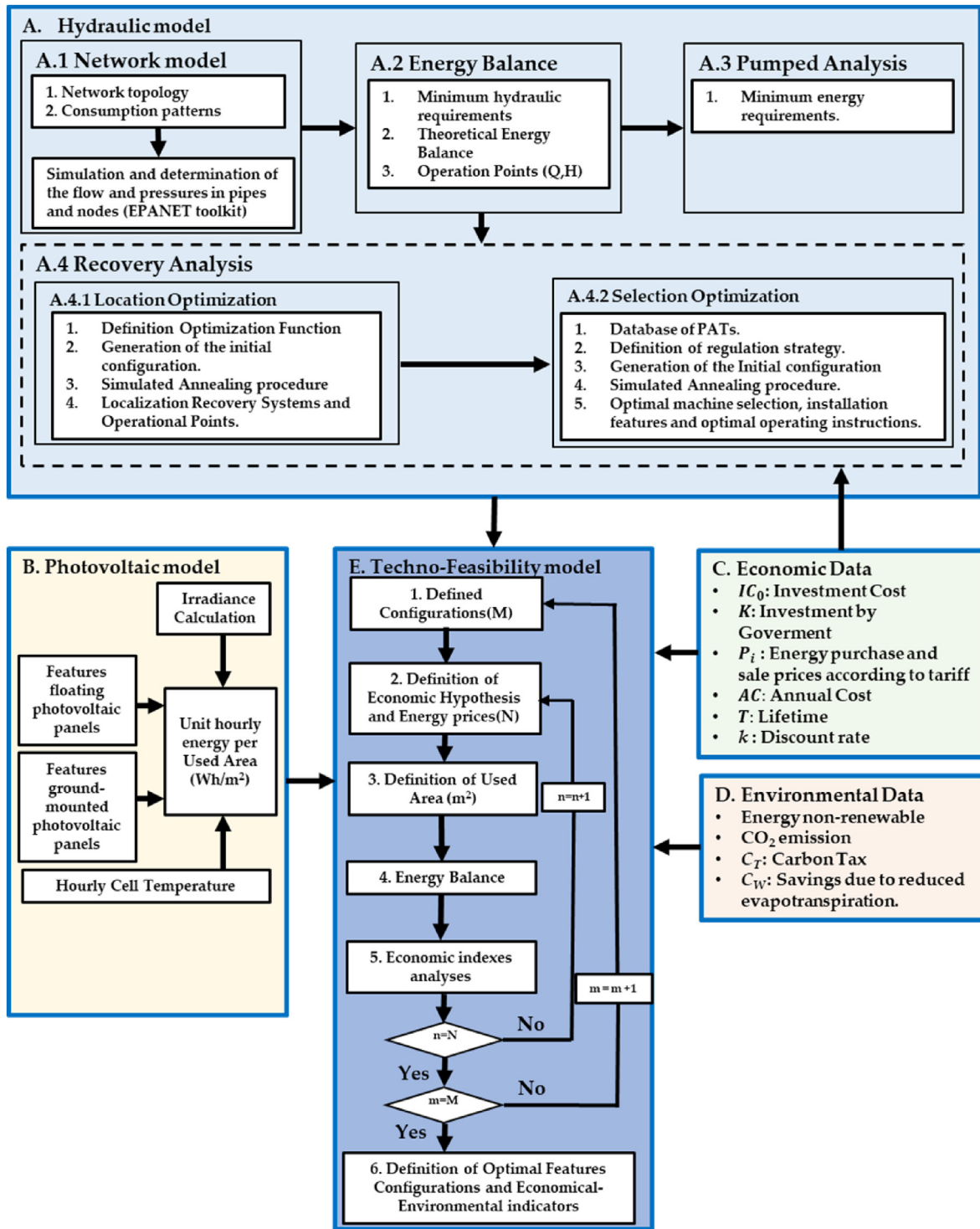


Fig. 2. Proposed methodology.

the energy balance. This has the goal to define minimum hydraulic requirements to guarantee the quality of the irrigation service. It enables the definition of theoretical energy balance as well as the operation points (flow and injected head) for the pumped area of the systems. The energy balance in the irrigation points is defined by the following expression, which was summarized by Ref. [48]. The model considers the annual balance of energy in each moment defined by Equation (1):

$$\sum_{b=1}^n E_{T_b} = \sum_{b=1}^n (E_{FR_b} + E_{RI_b} + E_{TR_b}) \quad (1)$$

where  $E_{T_b}$  is the total energy, which is supplied in the system in kWh considering the  $n$  irrigation points. This energy considers both supplied energy by gravity as well as the needed energy supplied by pump stations;  $E_{FR_b}$  is the friction energy dissipated by losses in



kWh;  $E_{Ri_b}$  is the required irrigation energy in kWh. It enables the knowledge of the minimum energy to satisfy the irrigation demand at a satisfactory level for the user;  $E_{TR_b}$  is the theoretical recoverable energy in kWh in this irrigation point. If the analysis point is a line, the water manager should consider also the theoretical non-recoverable energy ( $E_{NTR}$ ) due to the topology of the network [48].

The knowledge of the operation flows enables the definition of the operation of the pumped systems (A.3). It allows water managers to define the regulation strategy of the pumps, and therefore, it establishes the energy needs of the system. Otherwise, the knowledge of the operation flows in the gravity system as well as the values of the theoretically available energy enable the recovery analysis using microhydropower systems. This analysis is considered in step A.4. This stage is focused on the recovery analysis and it is defined by two different stages. The first stage, called A.4.1 Location optimization, is established by five different stages: (i) Definition Optimization Function; (ii) Generation of the initial configuration; (iii) Simulated Annealing procedure; (iv) Localization Recovery Systems; and (v) Operational Points.

The optimization procedure was developed using WaterPAT software, which was programmed by the authors. The schematic procedure of the simulated annealing is defined in the following figure.

Fig. 3 shows the different steps. An ordered list of the elements, which want to be optimized is generated. The order is established according to the energy balance defined by the objective function. The algorithm uses different parameters as initial temperature ( $T_i$ ), the final temperature ( $T_f$ ), cooling ratio ( $\alpha$ ) and number of transitions for each temperature step ( $L_0$ ). A sensitivity analysis is developed previously to improve the optimization. The transition temperature ( $T_t$ ) is calculated according to a geometrical relation, which is defined by a  $\alpha$  coefficient. The range of the parameters is

defined between 2 and the maximum number of lines in the supply system. The simulated procedure defines new combinations between different  $m$  elements. It stops when it reaches the optimum configuration for the  $N$  system. The procedure is completely defined and evaluated by Ref. [41].

The simulated annealing is developed using the Levelized Cost of Energy (LCOE) [49]. It is used as the optimization function to be minimized. This function only takes into account expenses (initial investment and annual costs) and it does not depend on energy prizes.

$$LCOE^R = \frac{IC_0^R + \sum_{i=1}^{i=T} \frac{AC_i^R}{(1+k)^i}}{\sum_{i=1}^{i=T} \frac{RE_i^R}{(1+k)^i}} \quad (2)$$

where  $IC_0^R$  is the initial investment in € in the year 0, considering the electric line to reach the supply points;  $AC_i^R$  is the operation and maintenance costs in € for the year  $i$ ;  $RE_i^R$  is the annual recovered energy in kWh for the year  $i$ ;  $T$  is the lifetime in years, considering 25 years since it coincides with the photovoltaic panels;  $k$  is the real discount rate using a sensitivity analysis between 0.01 and 0.1. The real discount rate included both nominal discount rate and expected inflation rate, similar to other software (e.g., HOMER) [50].

When the optimization function is defined, the simulated annealing is applied. It establishes the initial configuration and runs the optimization procedure. This procedure was defined and applied by Ref. [41]. The solution of the simulated annealing determines the best locations of the recovery systems, considering the different pipes and the different optimization functions. When the location is finished, the methodology continues to choose the best machine (A.4.2). The selection of the machines contains the second optimization procedure. This optimizes by simulated annealing and the model searches for the best machine to be installed in the previous optimized location, which defines the available operation points.

This step is defined by five different steps, which are focused on: (i) establishing the database machine, (ii) Definition of the regulation strategy. This sub-step defines the operation mode of the machine. It can choose between non-variation rotational speed or variable rotational speed. When the variation rotational speed is considered, different strategies are analysed: best power head (BPH), best efficiency head (BEH) and best power flow (BPF) [51]; (iii) the initial configuration is defined according to (i) and (ii); (iv) the simulating procedure is developed; (v) the best solution is established in terms of the optimization function and the different variables to choose the number of machines, flow regulation per machine and recovered head depending on the selected optimal strategy.

When block (A), which performs on the hydraulic system, establishes the real recovered energy using hydropower, the second block starts if the consumed energy is higher than generated energy. The second block (B) is focused on the get the maximum energy by solar irradiance by square meter. The block is defined by four different sub-blocks. The first sub-block establishes the calculus of the hourly irradiance along the year. It improves the analytical model proposed by Ref. [31]. From the angle of latitude, day of the year, angle of declination, and angle of sunset time, the extra-terrestrial irradiation incident on a horizontal plane is calculated. With this value, the ratios for diffuse radiation and direct radiation are obtained. From the sunrise and sunset times, assuming an isotropic sky, it is possible to calculate the diffuse, direct and global hourly irradiance components as a function of the tilt angle of the panel. It is necessary to know the geometrical characteristics of the panels and floating systems, to determine the installed power, performance decay, minimum distance between panels and ratio between the installed area and the used area.

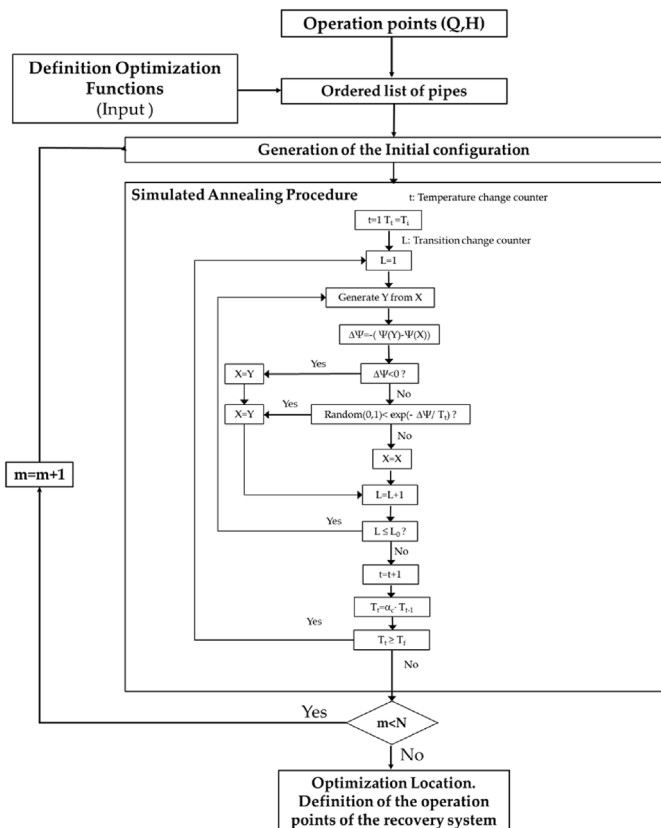


Fig. 3. Example of one of the simulated procedures applied to the methodology.

Finally, it calculates the performance from the hourly average temperature.

The equation modelling for the GPV system, which is integrated into the proposed methodology is described and developed by Ref. [31]. The methodology used the equations modelling developed by Ref. [52] when the FPV systems are integrated with the optimization procedure. The PV analysis used a performance ratio equal to 0.7 to include the different efficiencies of the panels.

The optimization procedure considers the installation of both GPV and FPV systems. FPV systems are installed on the free water surface of the different reservoirs to use this area. This solution was proposed by Ref. [17]. The optimization module considers: the characteristics of the photovoltaic panel using a database, the same for both fixed and floating; floating system characteristics using the patented inclination equal to 5° [53]; the tilt angle is left variable for the ground-mounted system and it is 5° for the floating system, cost and energy production are simplified as a function of the used area. The analysis of output power of FPV and GPV is different since the installation of the PV panels is different. The analysis of the PV areas is a function of the available surface both reservoir and ground. The use of the water surface of the reservoir is to take advantage of these areas as well as to decrease the water losses by evaporation, which can be reduced by between 33 and 50%. Although the FPV power is higher due to lower cell temperature, The research does not consider this phenomenon, being on the side of safety in the estimation of the generated powers [54].

The third block (C) is the economic analysis. This block has implications for both blocks A and E (Fig. 2) to develop the selection of the machines as well as the final feasible optimization analysis. This block defines the feasibility of the system. The economic analysis considers different ratios and prizes used by others published research. The goal of this section is the establishment of the economic ratio to use in the optimization procedures and making decision tools. Table 1 shows the different used values as well as the references.

The fourth block (D) is focused on the analysis of the environmental impact of the solution in the system. This block analyses the non-renewable energy resource according to Ref. [69], the greenhouse emissions for this resource as well as the economic impact of these CO<sub>2</sub> emissions. The analysis of the non-renewable energy ( $E_{NRE}$ ) use is defined energy coefficient (EC), which is defined by the follow expression proposed by Ref. [69].

$$E_{NRE} = EC \cdot E_c \tag{3}$$

where EC is the coefficient, which relates between energy generated by non-renewable resources and consumed energy in the system. It is equal to 1.954;  $E_{NRE}$  is the non-renewable energy resource in kWh,  $E_c$  is the consumed electrical energy in the system by the grid in kWh.

The CO<sub>2</sub> emissions value (CO<sub>2</sub>E) caused by this generation could be estimated according to the following expression [70]:

$$CO_2E = CO_2C \cdot E_c \tag{4}$$

where CO<sub>2</sub>C is equal to 0.331 kgCO<sub>2</sub>/kWh [71], CO<sub>2</sub>E is the CO<sub>2</sub> emissions in. kgCO<sub>2</sub>

These emissions are punished by a tax, which is established considering a value proposed by Ref. [66]. This carbon tax ( $C_T$ ) enables the definition of the profit for the use of renewable energies or the punish for the consumption non-renewable energies. The economic value can be defined by the following expression:

$$CO_2C = C_T \cdot CO_2E \tag{5}$$

Where CO<sub>2</sub>C is the cost/profit in € for the environmental profit;  $C_T$

is the carbon tax. It is equal to 0.1162 €/kg CO<sub>2</sub>. This  $C_T$  considers an annual increase equal to 3% according to Ref. [72].

Finally, block E defines the making decision stage, which develops the techno-feasibility model. This block develops the study of the different approaches and possible configurations (M), which could be defined in the management system. The different configurations are defined in Table 2.

The six configurations included in the methodology are: (A) Pumped system; the methodology can consider there are pump stations in the water system, and therefore, it considers the energy need to supply the different pumped areas; (B) Recovery system; the methodology studies the possibility to install the different recovery systems according to block A, which was defined previously; (C) FPV, the methodology considers the possibility to install floating photovoltaic systems in the reservoirs of the system; (D) GPV, the methodology considers the possibility to install a ground-mounted photovoltaic system, (E) Batteries (off-grid); the methodology defines the connection to the grid, which enables the energy sales or (F) it does not consider the batteries use and the system is connected to the grid.

The feasible model establish for each configuration different analyses included six different steps. The definition of the configuration continues, considering the different economic hypotheses, including the energy price of both purchase and sale. The model considers three discount rates (0.01, 0.04, 0.07), two different energy block prices as a function of the time (i.e. current and future prices). Besides, the procedure should carry out the following constraints when the configuration considers the use of a storage system. The model considers a lifetime of twenty-five years, which is coincided with the lifetime of the PV systems. The model considers that in the optimization the properties of the battery remain constant throughout its lifetime and are not affected by external factors such as temperature, similar to other optimization software [50]. However, when there are charge/discharge cycles, the capacity decrease of these elements. To consider this factor, the model defined an increased coefficient of 1.25 to take into account the loss of battery capacity and therefore indirectly include it in the feasible analysis.

The model considers the different used areas to optimize the photovoltaic area both FPV and GPV. Different combinations can be chosen considering the area and the inclination angle when the photovoltaic system is on the ground and the different areas when the photovoltaic system is floating. The analytical model enables the definition of the best solution by comparing the Net Present Value (NPV) between the situation without recovery and photovoltaic installation with the situation defined by the configuration and hypotheses. The procedure calculates the economic savings according to the following expressions [73]:

$$NPV_0^I = \sum_{i=1}^{i=T} \frac{-AC_i^I}{(1+k)^i} \tag{6}$$

$$NPV_m = -IC_0 + \sum_{i=1}^{i=T} \frac{(AI_i - AC_i)}{(1+k)^i} \tag{7}$$

$$\Delta NPV = NPV_m - NPV_0^I \tag{8}$$

$$S = \frac{\Delta NPV}{NPV_0^I} \cdot 100 \tag{9}$$

Where  $NPV_0^I$  is the Net Present Value without recovery and photovoltaic installation in €,  $AC_i^I$  is the annual cost, including operating and energy costs in €,  $NPV_m$  is the Net Present Value for

**Table 1**  
Economic costs used in the optimization procedure.

Investment Cost	
Injected and Recovery Systems	$IC = \sum IC_j$
	$IC_{CD}$ Control Device. Electric and Electronic devices for the control of the system 0.24 · IC [55]
	$IC_{OPC}$ Other Project Cost including Engineering, Taxes 0.19 · IC
	$IC_{Civil}$ Civil works $1020 \left(\frac{\text{€}}{\text{kW}}\right)$ [56]
	$IC_{PATs}$ Hydraulic and motor/generator Cost $350 \left(\frac{\text{€}}{\text{kW}}\right)$ [57]
	$IC_{CV}$ Control Valves $C(\text{€}) = AD(\text{mm})^a$ A = 0.028 a = 1.86 [58]
	$IC_{PRV}$ Pressure Reducing Valve A = 1.34 a = 1.32
	$IC_{Pipe}$ Pipe Cost A = 0.218 a = 1.053
	$IC_{FM}$ Flowmeters A = 0.195 a = 1.59
Ground-mounted Photovoltaic	$IC_{GPV}$ Solar Panels and installation 700 €/kW [59]
	$IC_{Soil}$ Purchase of rural land 10000 €/Ha
Floating Photovoltaic	$IC_{FPV}$ The floating structure, not including Solar Panels and installation $54.69 \frac{\text{€}}{\text{m}^2} (\beta = 5^\circ)$ [60]
Joint investment	$IC_{Connection}$ Electrical connection $25500 (\text{€}) + 77 \left(\frac{\text{€}}{\text{m}}\right) \cdot L(\text{m})$ [56]
	$IC_{Battery}$ Batteries. Replacement for half of the study years, for 60% of the current price. 518.8 €/(kWh) [61]
Investment Government	K The ratio of the investment supported by Government Hypothesis 1: K =0 [62]
Investment Government	Hypothesis 2: K =0.5
Annual Income	
Joint annual income	$IC_{Sales}$ Energy sales For all tariff periods: [63]
	Current Energy prices:
	Power installed: 0 €/kW
	Energy prices: 0.05 €/kWh
	Future Energy prices:
	Power installed: 0 €/kW
	Energy prices: 0.10 €/kWh
	Production Tax: 7%
	Access Tax: 0.0005 €/kWh
Annual Cost	
$AC = \sum AC_j$	
Injected and Recovery Systems and Joint Investment	$AC_{OMEX}$ Operational and maintenance cost 0.1 · IC [64]
Ground Mounted and Floating Photovoltaic	$AC_{OMEX}$ $15 \frac{\text{€}}{\text{kW} \cdot \text{year}}$ [65]
Joint annual Cost	$AC_{Purchase}$ Energy purchase Depending on the tariff period: [63]
	Current Energy prices:
	P1-0.106938 €/kW 0.1295 €/kWh
	P2-0.053515 €/kW 0.1195 €/kWh
	P3-0.039164 €/kW 0.1124 €/kWh
	P4-0.039164 €/kW 0.1069 €/kWh
	P5-0.039164 €/kW 0.1031 €/kWh
	P6-0.017869 €/kW 0.0996 €/kWh
	Future Energy prices:
	Double the current prices
	Purchase Tax: 5.11269632%
	Renting the electricity meters: 50 €/month
Environmental Data	
Carbon emissions	$C_T$ Carbon Tax. A growth rate of 3% per year is assumed 116.2 €/TnCO <sub>2</sub> [66,67]
Floating Photovoltaic	$C_W$ Savings due to reduced evapotranspiration $1 \frac{\text{€}}{\text{m}^3}$ [68]

**Table 2**  
Definition of the different configurations.

Element	Configuration					
	A	B	C	D	E	F
<b>Pumped</b>	Analysed	Analysed	Analysed	Analysed	Analysed	Analysed
<b>Recovery System</b>	Analysed	Analysed	Analysed	Analysed	Analysed	Analysed
<b>FPV</b>	Not Analysed	Not Analysed	Analysed	Analysed	Not Analysed	Not Analysed
<b>GPV</b>	Not Analysed	Not Analysed	Not Analysed	Not Analysed	Analysed	Analysed
<b>Batteries</b>	Analysed	Not Analysed	Analysed	Not Analysed	Analysed	Not Analysed
<b>Connected to grid</b>	Not Analysed	Analysed	Not Analysed	Analysed	Not Analysed	Analysed

GPV.- Ground-mounted Photovoltaic System; FPV.- Floating Photovoltaic system.

the defined configurations and assumptions in €, according to  $IC_0$  investment cost in €,  $IC_i$  annual cost including operation and energy purchase (depending on the configuration) in € and  $AI_i$  annual revenue from energy sales in €,  $\Delta NPV$  is the difference of Net Present Values in €;  $S$  is the percentage of economic savings; if  $NPV_m > NPV_0^I$  then  $S > 0\%$ , if  $NPV_m < NPV_0^I$  then  $S < 0\%$ , if  $NPV_m = NPV_0^I$  then  $S = 0\%$ , and if  $NPV_m = 0$  then  $S = 100\%$ .

The procedure defines two minimum areas. The first area defines the minimum value for getting  $S = 0\%$  and the second area defines  $S = 100\%$ . For GPV, the minimum areas are defined as a function of tilt angle. The techno-feasible model studies the different feasible analyses including the energy balance by an iterative procedure. It considers different values of the farmed areas in the irrigation system since the facilities cannot define an optimized farmed area because the farmed area depends on other social and economic factors linked to agriculture. It causes the water management can know the minimum areas to reach hybrid systems, which will feasible the self-consumption in energy terms.

The techno-feasible analysis includes the temporal analysis of the different environmental ratios, which show the support of each renewable system for the necessary energy. The following ratios are analysed in the final balance:

- Self-Consumption Index (SCI) is the ratio between renewable energy, which is consumed in the pump station and the needed energy.
- Recovered Ratio (RR) is defined as the ratio between recovered energy by microhydropower system and the necessary energy by the pump stations
- Photovoltaic Ratio (PVR) is defined as the ratio between generated energy by the photovoltaic systems (GPV or FPV) and the necessary energy by the pump stations.
- Recovered Energy Sales Ratio (RESR) is the ratio between recovered energy, which is sold to the grid and the total recovered energy by the microhydropower system.
- Photovoltaic Sales Ratio (PVSr) is the ratio between generated photovoltaic energy, which is sold to the grid and the total generated energy by the photovoltaic systems.

- Purchased Energy Ratio (PER) is the ratio between purchased energy to the grid and the necessary energy for the pump station
- Recovery Energy Ratio (RER) is the ratio between microhydropower energy used for the pump station and the necessary energy for the pump station.
- Photovoltaic Energy Ratio (PVER) is the ratio between photovoltaic energy used for the pump station and the necessary energy for the pump station.
- Reduction of the CO<sub>2</sub> emissions (RCO<sub>2</sub>) is the estimation of the decrease of CO<sub>2</sub> emissions, considering the renewable energy generated by the hybrid renewable system.

### 3. Results

#### 3.1. Case study

The water system is located in Aspe (Alicante, Spain). The water system supplies 3708 ha in which the main crop is the table grapes. The irrigation system is pressurized and the level of the crops was located between 395 m and 211 m. There were four reservoirs, which supply the different sectors of the pressurized system. The main reservoir (R-1), which is located at level 384.5 m receives the irrigation water, which comes from different sources (well and Jucar-Vinalopó transfer mainly) [74]. R-1 distributes the water between different reservoirs by gravity. There are two high zones, which should be pumped to guarantee the minimum pressure and therefore the demanded flow in the system. It implies the need to operate with two pump stations (P-1 and P-2 respectively). The irrigation network was simulated using EPANET, which was calibrated according to the proposed methodology by Ref. [75]. (see Fig. 4)

The high difference levels between irrigation points enable the possibility to install recovery systems in the irrigation network. Besides, the high surface of the reservoir enables the possibility to install a floating photovoltaic system to generate green energy, reducing the water losses in the reservoir as a consequence of water evaporation. Both pumped stations are near the reservoirs, which are called R-1 and R-2 respectively. The water network is built on ductile iron, although there are short branches, which are built using high ductile polyethylene (HDPE). The total pipe length is 274 km and the diameters are between 31 mm and 1200 mm. The

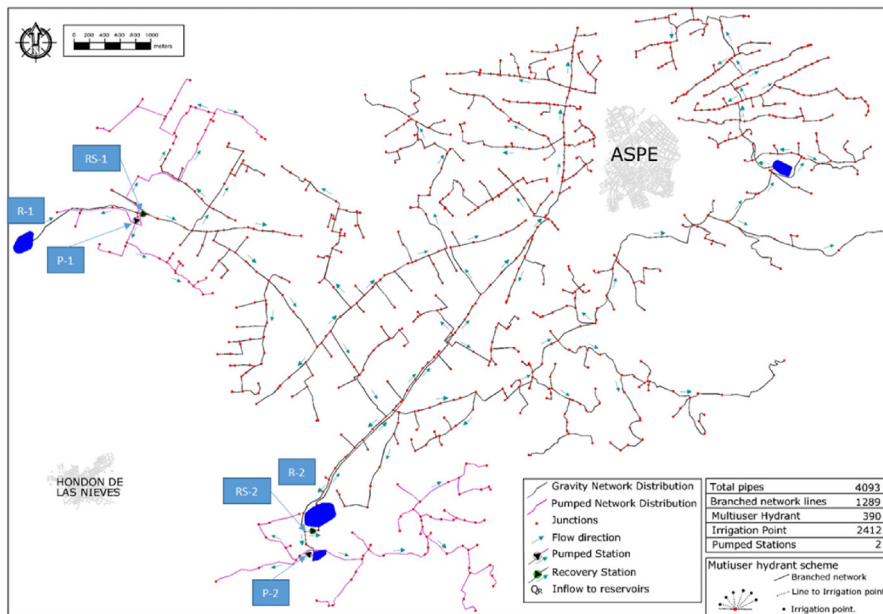


Fig. 4. Case study (ETRS89 UTM 30S 694899E 4246291N).  
860



installation has 390 multiuser hydrants in which the pipes are connected by a manifold to supply the irrigation points using polyethylene pipes. P-1 station is defined by three pumps in parallel. The best efficiency point of these machines is 111 l/s and 50 m w.c., being the efficiency equal to 0.83 and its nominal rotation speed 1760 rpm. In contrast, the P-2 station is defined by three pumps in parallel. The best efficiency point of these machines is 120 l/s and 53 m w.c., being an efficiency equal to 0.79 and its rotational speed 1760 rpm. The main characteristics of the pumped stations are defined in Appendix 2 in Table 1.

The analysis includes different scenarios, which considered different values of the farmed area since the analysis cannot consider an optimum farmed value. It is because the farmed area does not depend on the feasibility of the energy system but on others constraints, which are linked to the agricultural production system such as prices, water availability, and social and environmental conditions. The farmed area depended on the other conditions linked to economical and social. Particularly, the methodology considered five hypotheses: 50%, 60%, 75%, 90% and 100% of the farmed area compared to the available irrigation area. The analysis of the pump systems establishes the need to develop the energy balance and the knowledge of the operation points of the systems. Besides, block A enables the optimization of the recovery system as well as the calculus of the energy balance when the recovery systems are located and the machines are selected. The following values were obtained in both pumped stations according to pumped and recovered values of energy, considering the irrigation needs between 2001 and 2020 [76] and analyzing the average temperature in the case study between 2007 and 2016.

Finally, to describe the data of the case study, Fig. 5 shows the average value of the solar irradiation for both systems (FPV and GPV) as well as the average temperature value.

The solar radiation varied between 0.12 kWh/m<sup>2</sup> (January) and 0.32 kWh/m<sup>2</sup> (July) when the GPV was analysed. The analysis of the solar radiation oscillated between 0.160 kWh/m<sup>2</sup> (January) and 0.280 kWh/m<sup>2</sup> (July) when FPV was studied. The average values of temperature oscillated between 6 °C and 25 °C from December and July respectively. The characteristic of the PV panels were defined in Appendix 2 (Table 2).

### 3.2. Selection machine optimization

If P-1 is analysed, the recovered energy using hydropower systems is greater than the consumed energy by the pump station between 50 and 75% of the farmed used. In this P-1 station, the annual excess of generated energy is around 24,000 kWh. When the farmed area increases above 75% the energy needs are higher in the P1 station, and the increase of the recovered energy by the circulating flows in the water network cannot compensate for it. In this assumption, the lack of energy to reach the zero-net consumption of non-renewable energy is around 26,800 kWh each year. When P-2 is analysed in similar terms, comparing energy needs in the P-2 station and the recovered energy, all assumptions showed a lack of green energy to reach the zero-net energy consumption. In this case, the lack of annual energy oscillates between 50,400 and 101,525 kWh from 50 to 100% farmed area, respectively. The lack of energy in the different assumptions establishes the need to complement using other renewable systems, particularly, PV panels both GPV and FPV.

Fig. 6 shows the different LCOE values when the optimization procedure was applied, considering different farmed areas between 10 and 100%, four different discount rates ( $k$ ) and a different number of installed recovery systems (NRS) from 1 to 10. When different rates are analysed, considering  $k = 0.01$  (Fig. 6a),  $k = 0.04$  (Fig. 6b),  $k = 0.07$  (Fig. 6c) y  $k = 0.1$  (Fig. 6d), the trend of all figures

is similar, the LCOE decreased between 70 and 80% as a function of the increase of the farmed area. If the NRS increased, the LCOE increased between 340 and 520%. Currently, the farmed area is around 75%. In this case, the LCOE value is between 0.38 and 0.58 €/kWh when two recovery systems are considered. These values are lower than published values, which were between 0.63 and 1.17 €/kWh by Ref. [77], using pump working as turbine. The optimized LCOE values decreased 50% compared with the published values. However, the LCOE reached uniform values when the farmed area was above 60%, showing variation lower than 0.05€/kWh.

Finally, two NRS were chosen according to the number of pump stations since the optimization procedure enables the installation of these recovery systems near pump stations. Fig. 7a shows the optimization carried out by the simulated annealing to choose the machines, which operate in each recovery system. For each recovery system, the simulated annealing procedure optimizes the number of installed machines in parallel. Particularly, two machines were the best solution for recovery system 1 (RS-1) and one machine for the recovery system (RS-2). Fig. 7a shows the LCOE value as a function of the specific speed ( $n_{st}$ ) for RS-1 and RS-2 when the farmed area was 50%. In this case, the LCOE value for this machine was 0.53 once the characteristic curves of both group machines are considered (Fig. 6d). The specific speed was 130 and 48 rpm (m, kW) for the machines RS-1 and RS-2. LCOE value was around 0.44 when the farmed area was 75% (Fig. 7b). In this case, the specific speeds of the optimized selection were 129 and 44 rpm for RS-1 and RS-2, respectively. Fig. 7c shows the values for 100% farmed area, reaching LCOE values near 0.33 and specific speeds of 136 and 38 rpm for RS-1 and RS-2, respectively. The optimization analysis showed that the typology of the machines did not change significantly when the farmed area varies. It implies the need to use axial machines for RS-1 and radial machines for RS-2.

### 3.3. Farmed area analysis

The consideration of the values for economic and environmental costs, which were defined in Table 1 enables the development of the feasibility analysis using the proposed methodology and the different configurations. Besides, the results show the feasibility values considering the current energy prices and estimating the future energy prices according to Ref. [63]. Each feasibility analysis shows results considering Fig. 8a shows the results when the P-1 and RS-1 are considered without the use of GPV and FPV (Configuration B according to Table 2). The results show the self-consumption is unfeasible for any discount rates, using micro-hydropower system in which the energy generation is higher than the energy necessary for the pumping. In contrast, if the future energy price is considered, self-consumption is feasible when the farmed area is higher than 70%. If the same analysis is developed in P-2 (Fig. 8c), when the RS-2 is analysed according to configuration B (i.e, without GPV and FPV), the green generation is feasible when the farmed area is higher than 80% for any discount rate and considering the current energy prices. When the feasible analysis considered the future energy prices, the self-consumption is feasible when the farmed area is greater than 50%.

If the study considers a public investment equal to  $K = 0.5$ , the self-consumption is feasible in P-1 when the farmed area is higher than 50% for any discount rates, considering the future prices (Fig. 8b), and the facilities are feasible when the farmed area is higher than 80%, considering the current energy prices. If P-2 is analysed (Fig. 8d) the savings are present in all ranges of the farmed area when it is higher than 60%, considering current and future energy prices. The figure shows the feasibility of the system according to techno-feasible analysis and therefore, it shows the possibility to reach a zero-net energy balance in the annual

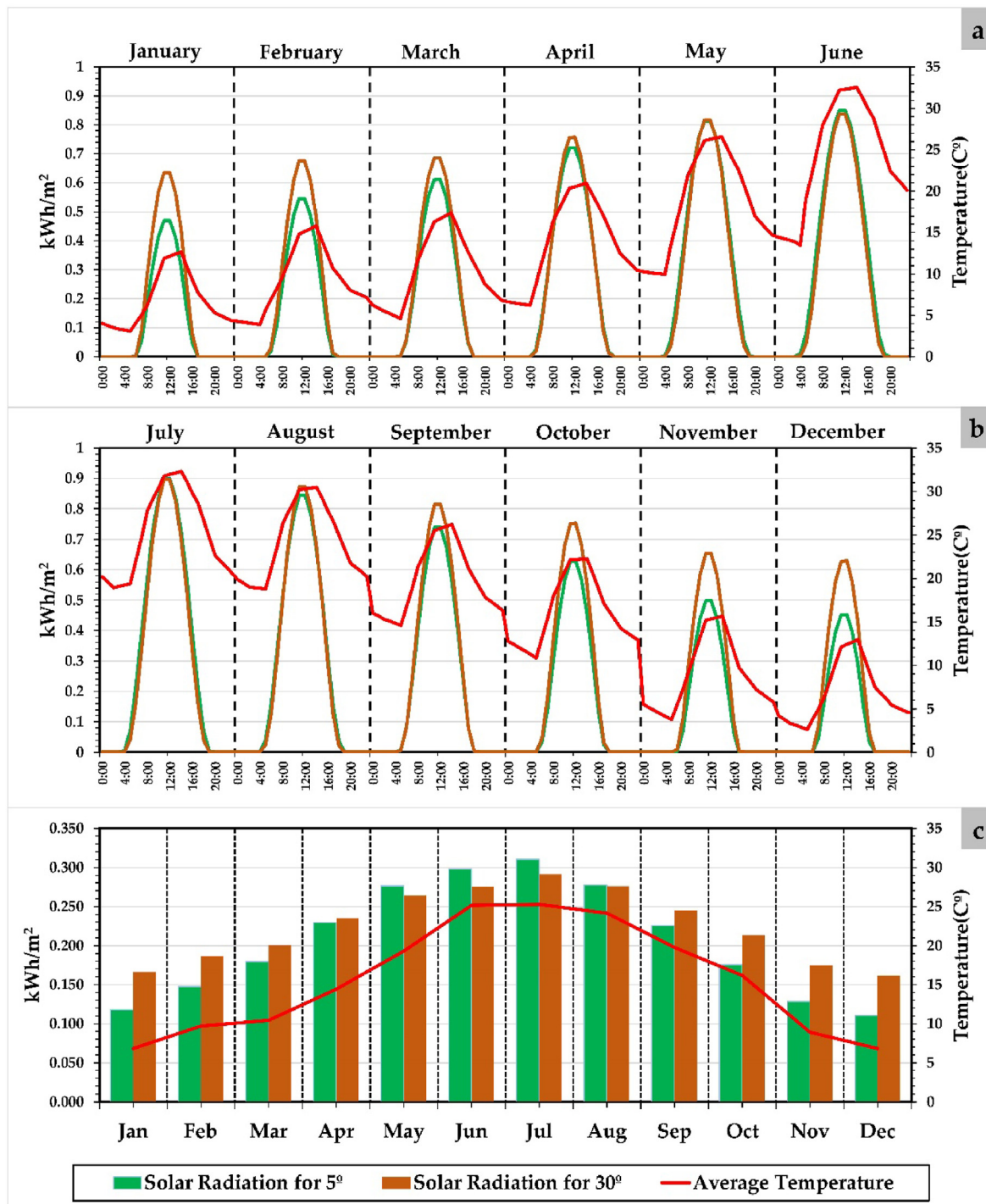


Fig. 5. Average solar radiation and temperature each month (a) Hourly between January and June; (b) Hourly between July and December; (c) Average each month.

operation system.

Fig. 9 shows different configurations when the GPV and FPV are considered in P-1. Fig. 9a shows the area necessary for FPV panels when configuration C is analysed. This configuration (Table 2) supposes the use of RS-1 supported with FPV panels in which the energy excess is stored using batteries. The advantage of FPV systems is the use of the water surface of the reservoir and therefore, the water management does not have to buy farmed area for the installation of the FPV system. Besides, the installation of the FPV

causes the evaporation decrease of the water in the reservoir. It causes the reduction of leakages costs, which were considered in the feasible analysis according to Table 1.

Fig. 9a shows the minimum area to reach an NPV equal to 0, considering future energy prices without public investment. When the farmed area is analysed, the FPV area is between 28,000 and 30,000 m<sup>2</sup> when the farmed area oscillates between 50 and 100% respectively, considering discount rates equal to 0.01. If the results for  $k = 0.01$  and  $k = 0.04$ , Fig. 9a shows the minimum FPV area to

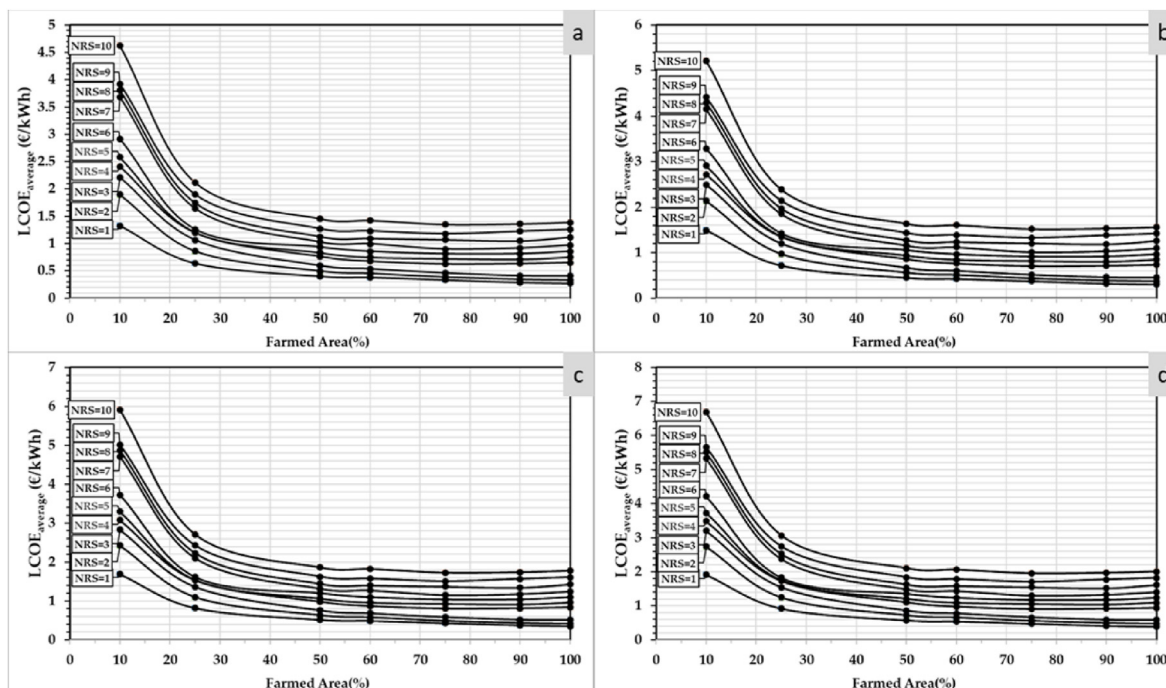


Fig. 6. LCOE values for different discount rates (k) (a)  $k = 0.01$ , (b)  $k = 0.04$ , (c)  $k = 0.07$ , (d)  $k = 0.1$ .

get savings considering the current energy prices and the public investment ( $K = 0.5$ ). If these results are observed in Fig. 9a, the variation of the FPV area is non-linear as a function of the farmed area. If the discount rate is 0.01, the FPV area varies from 10,000 to 7000 m<sup>2</sup>, while the farmed area change between 50 and 100%. If the discount rate is 0.04, this FPV area oscillates between 25,000 and 12,000 m<sup>2</sup> for the farmed area of 50 and 100% respectively. The trend is similar when the configuration D is analysed (Fig. 9b), the used area for the installation of FPV is reduced between 7.8% and 28% as a function of the minimum area for NPV = 0 considering future prices, or the minimum area to create savings considering the current energy prices and different discount rates (Fig. 9b).

The configurations E and F analysed the use of GPV instead of FPV. The trend of these configurations is similar for configurations C and D, although the used areas change for the installation of the GPV when different energy prices and different discount rates. In general terms, the GPV areas and FPV areas are similar when the current prices are used and the discount rate is 0.01. Similar values and trends were obtained when the P-2 system was analysed considering the different configurations and economical hypotheses.

### 3.4. Energy balance and renewable share analysis

Once the best solution is chosen by the optimization procedure, the annual energy balance can be estimated each hour considering: (i) the consumed energy by pump station discretizing the tariff period, which changes between six different prices from P1 to P6 as a function of the day and month of the year (Table 1); (ii) the recovered energy by the excess of the hydraulic pressure in the system using microhydropower system; (iii) the generated energy by FPV/GPV panels installed in the system. Fig. 10a shows the annual energy balance in the P-1 system when the farmed area was 75%. In this case, the annual consumed energy by the pump station (injected into the network) was 103,387 kWh, the annual generated by PATs was 131,572 kWh, and the annual generated by the GPV panels was 243,844 kWh. These values showed an annual positive

balance equal to 283,125 kWh (connected to the grid or stored in batteries when the system is off-grid) and an annual negative balance equal to 10,187 kWh (the energy should be bought in the grid or supplied using batteries).

Fig. 10b shows the discretized hourly values for injected, recovered and generated energies on some days of July, as well as the hourly balance defining if there is excess or deficit of energy to supply the pump station. Besides, this figure indicates the tariff period in which the pump station is operating to define the saving of the energy consumption. Except in singular hours, there is an excess of the generated energy by the renewable system, showing the capacity of the system to sell or store energy. Particularly, the maximum excess was 1989 kWh and the maximum deficit was 186 kWh in this date window (14–17 July). Fig. 10c shows the hourly energy values, considering the GPV is disconnected to the P-1 because the generated energy using PATs is enough to satisfy the injected energy demand. In this case, the results show the lack of generated energy by GPV and all green energy is generated by the recovered systems. The injected values are lower than in July (Fig. 10b) due to irrigation needs decreasing for the grapes in November. In this stage, the excess energy was 1534 kWh and the maximum deficit was 29 kWh.

Fig. 11a shows the SCI and PVR values for three different scenarios of farmed areas as a function of the used area when there were installed GPV systems in the P-1 system. It shows the minimum SCI value is 0.35, without GPV and considering 50% of the farmed area. The self-consumption increases 71% and 85% when the farmed area was 75 and 100%, respectively. It indicates the high recovery potential when there are microhydropower systems, which take advantage of the excess pressure in the network, contributing to a decrease of leakages in the network. The inclusion of the GPV showed capacities to generate the necessary energy, which increased linearly from 0 until 60 when the farmed used area was 45,000 m<sup>2</sup>, The RR oscillated between 1.47 and 0.82 for 50% and 100% farmed area. Both high values PVR and RR showed enough capacity to generate by green renewable energies the necessary energy but the SCI cannot be 1 because the generation is dislocated



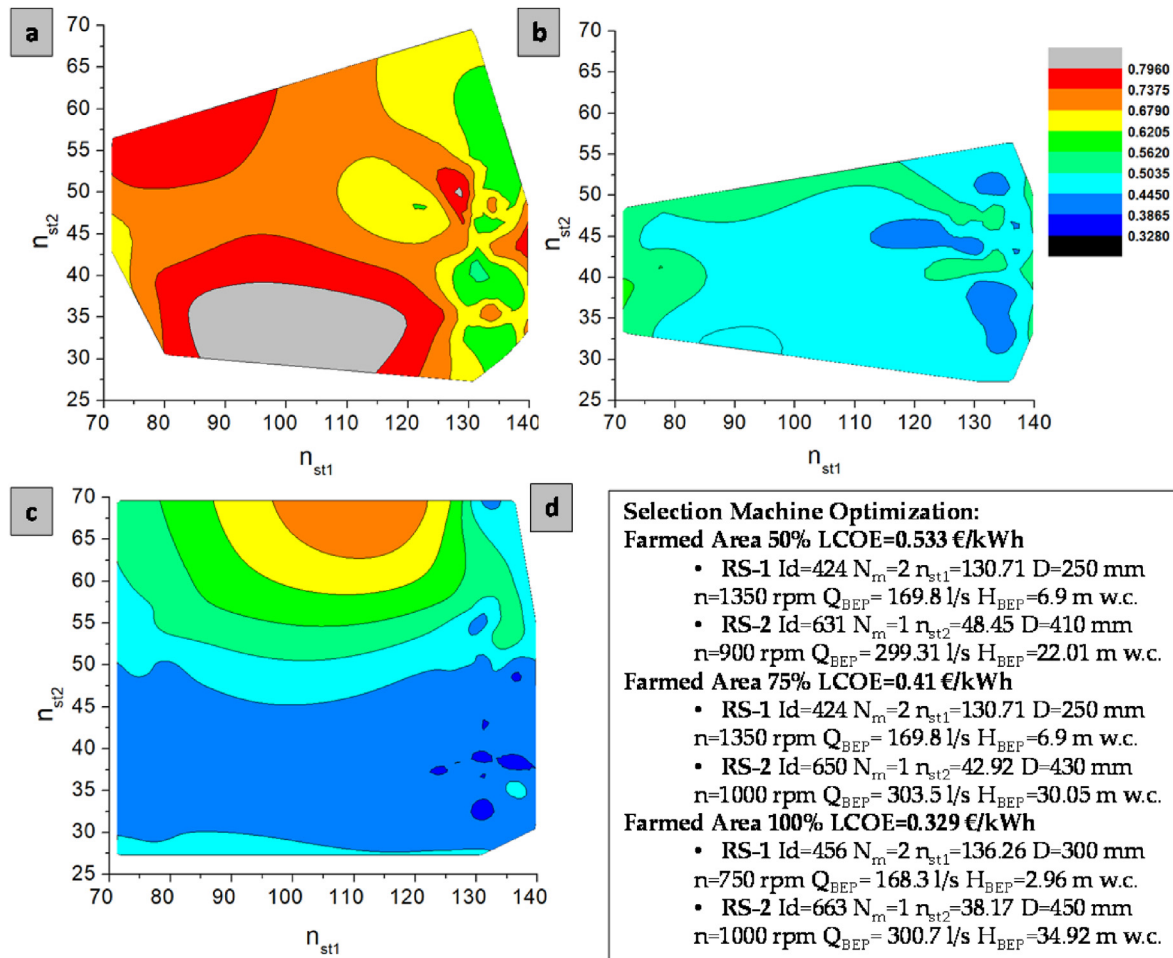


**Fig. 7.** LCOE average values ( $k = 0.04$ ) for different farmed Areas (a) 50%, (b) 75%, (c) 100%, (d) Characteristics parameters of the chosen machines in the optimization procedure (Id- Identification of the machine in the database; N<sub>m</sub>-number of installed machines; D- Diameter of impeller; n- rotational speed; n<sub>st1</sub>- specific speed of the R-S1; n<sub>st2</sub>- specific speed of the R-S2; Q<sub>BEP</sub>- Flow for the best efficiency point; H<sub>BEP</sub>- Recovered head for the best efficiency point of the machine).

of the demanded energy. The annual decrease of CO<sub>2</sub> emissions reached above 1400 Tones, which varied linearly according to the GPV area (Fig. 11b).

When the P-2 system was analysed the annual average SCI value was 0.83, the RR value was around 0.65 for any farmed area above 50%. In this case, PVR linearly increased between 15 and 32 as a function of the farmed area, considering a similar trend of the P-1 system. RESR oscillated between 0.69 and 0.49 for the P-2 system when the farmed area was analysed between 50% and 100%, respectively. Finally, the RER value varied between 0.20 and 0.33 for the P-2 system when the farmed area was analysed between 50% and 100%, respectively.

Fig. 11b shows the PVSR, PVR, PER and RCO<sub>2</sub> values of the P-1 system. PVSR and PVER values increased exponentially reaching values around 0.98, 0.94 and 0.83 for PVSR when the GPV area was 5000 m<sup>2</sup> and the farmed area were 50%, 75% and 100% respectively. PVER showed values of 0.23, 0.31 and 0.48 when the farmed area was 50%, 75% and 100% respectively, considering a GPV area of 5000 m<sup>2</sup>. The PER values were 0.16, 0.1 and 0.09 when the farmed area was 100%, 75% and 50% respectively. All values were asymptotic when the area increased for these values. If P-2 system was analysed, PVSR and PVER values increased exponentially reaching values around 0.88, 0.86 and 0.78 for PVSR when the GPV area was 5000 m<sup>2</sup> and the farmed area were 50%, 75% and 100% respectively. PVER showed values of 0.41, 0.43 and 0.53 when the farmed area

was 50%, 75% and 100% respectively, considering a GPV area of 5000 m<sup>2</sup>. The PER values were 0.25 approximately for any farmed area value.

Fig. 11c shows the values discretized by months, considering 10,000 m<sup>2</sup> of GPV system. The annual balance showed the SCI oscillated between 0.61 and 0.97 in January and July respectively, showing an annual average of 0.93. The total self-consumption was not possible, although the system showed the capacity to generate more energy of the necessary showing average values of PVR and RR of 1.28 and 9.52, respectively. It implied the sales could do in all months. PVSR varies between 0.90 and 1 in July and November, being the annual average 0.97. RESR showed high variability caused by the irrigation needs of the crops. These values were between 0.17 and 0.77 for July and November respectively, being the annual average of 0.53.

Fig. 11d shows the ratios of RER, PVER and PER, which define the origin of the necessary energy for the P-1 system each month. The minimum RER value was 0.27 in January, being a maximum of 0.86 in November. It shows the high potential of the recovery system to supply the pump station. The PVER oscillates between 0.06 and 0.45 for November and February, respectively. The annual average value was 0.33. Finally, the energy purchase (PER) oscillated between 0.03 and 0.37 for May and January, respectively. The annual value was 0.07 when the P-1 system was analysed.



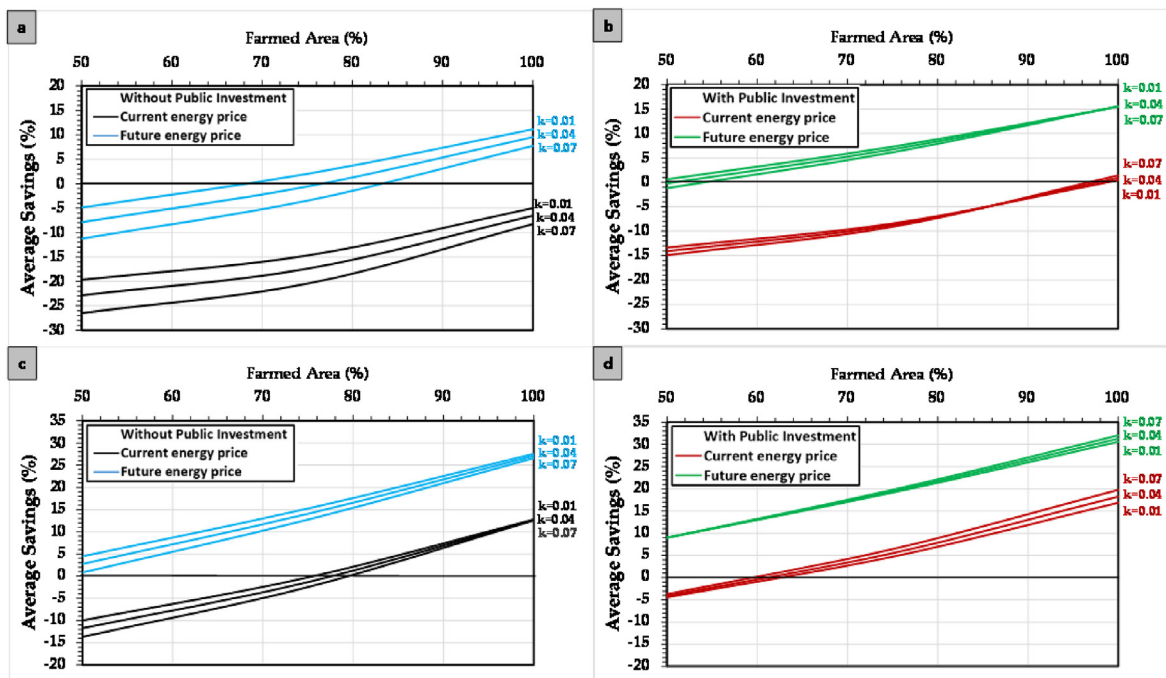


Fig. 8. Average savings according to the farmed area and discount rates for configuration B (a) P-1 no considering public investment, (b) P-1 considering public investment; (c) P-2 no considering public investment, (d) P-2 considering public investment.

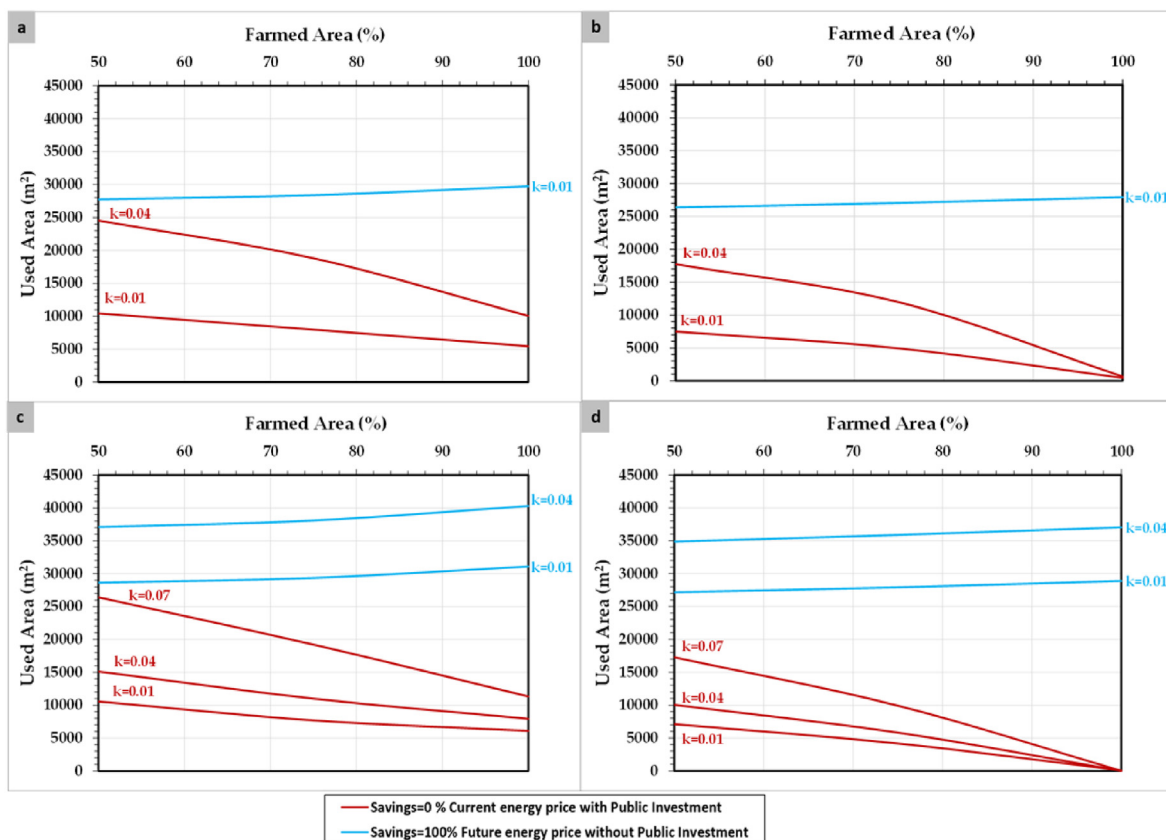


Fig. 9. Used area of photovoltaic systems for different discount rates and energy prices in P-1 (a) Configuration C, (b) Configuration D, (c) Configuration E, (d) Configuration F.

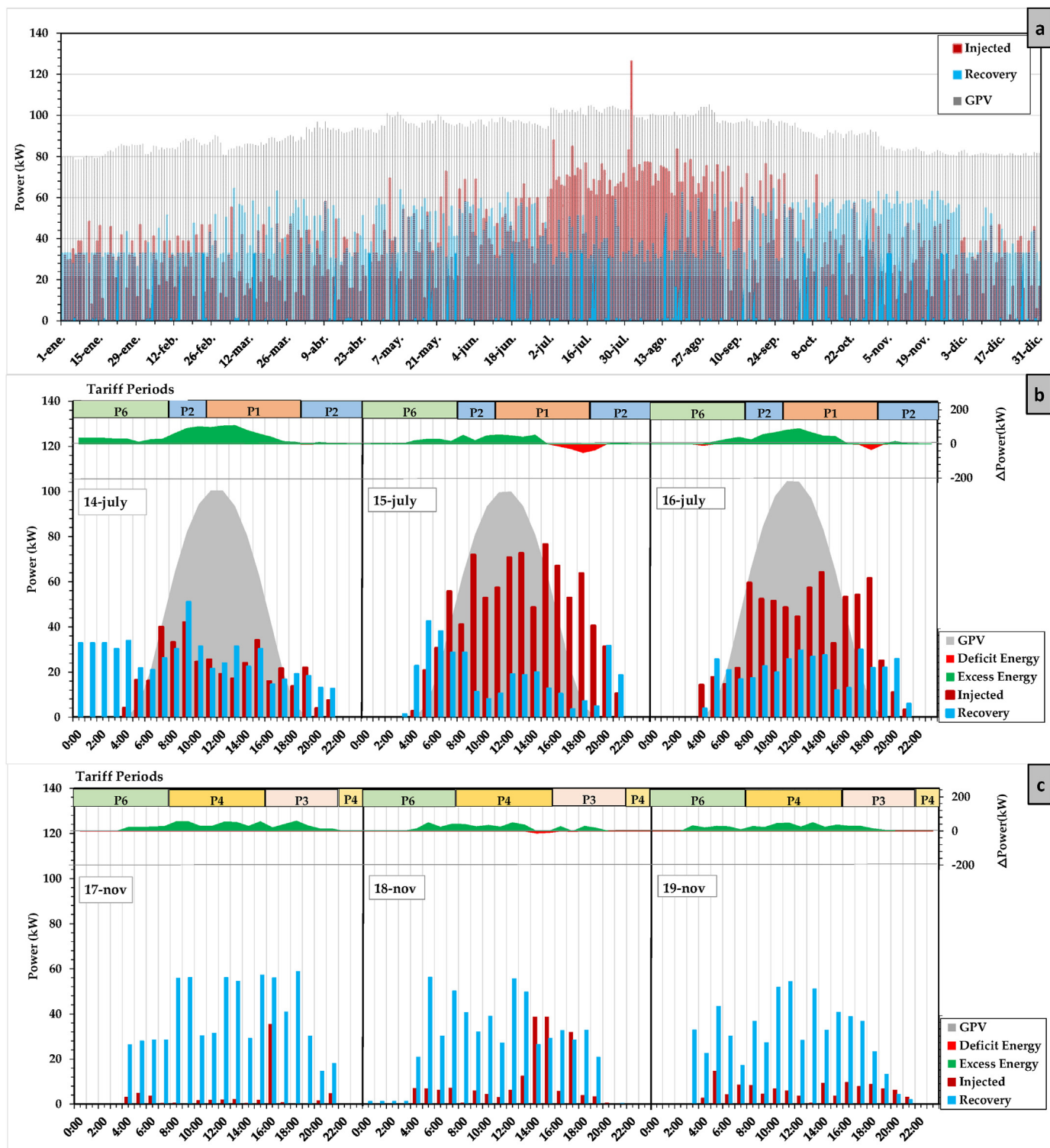


Fig. 10. Annual Energy balance considering GPV, microhydropower system and injected energy by the pump when P-1 system is analysed and the farmed area is 75%. (a) Annual (b) Hourly example between 14th and 16th July for configuration E or F; (c) Hourly example between 17th and 19th November for configuration A or B.

### 3.5. Discussion on the optimum solutions

Appendix 03 shows an analysis of the different obtained LCOE values when different configurations, different real discount rates, the energy prices (current and future) and the consideration of the possible public investments in both pumped systems (P-1 and P-2).

The table shows the combinations in the different configurations in which the use of hybrid systems is not feasible (it is defined by (a) in the different cells of the table). Table shows LCOE values, which are inside of the obtained values in other published researchers [77] and European reports [78]. These LCOE values considered the maximum area of the reservoir both R-1 and R-2, 45,000 and

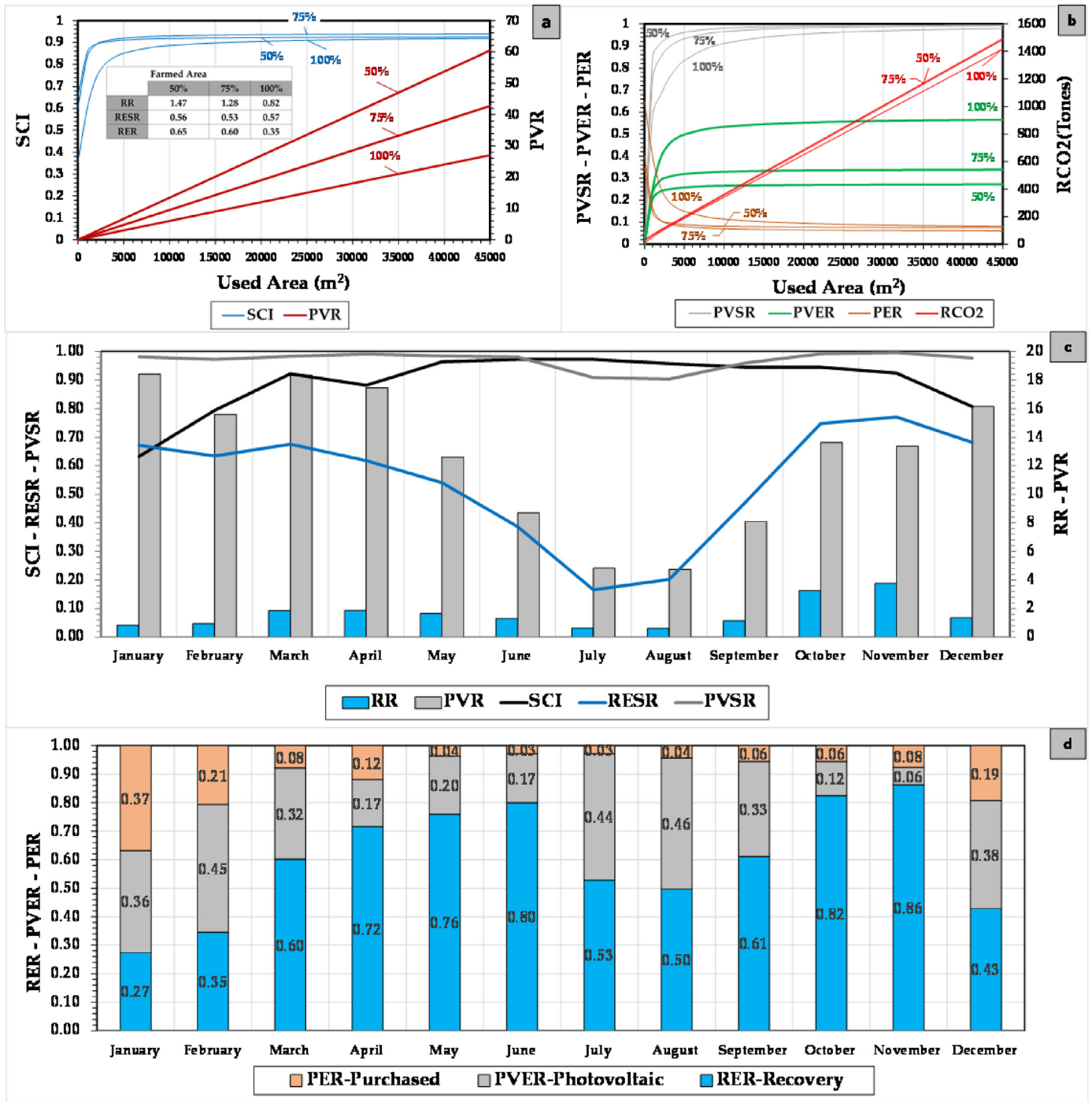


Fig. 11. Indicator values as a function of the farmed area when P-1 system is analysed for configuration F (a) SCI-PVR values (b) Annual Energy balance considering GPV, microhydropower system and injected energy (c) Monthly environmental indicators (d) Sales and Purchases ratios for each month.

80,000 m<sup>2</sup>, respectively. These areas are considered by the different scenarios to get the LCOE values. These values are marked using (b) and (c), respectively. The analysis showed the increase of energy in the future, will be these hybrid systems could be feasible without considering public investments, and the use of different discount rates did not cause significant differences between LCOE values. The increasing trend of the energy prices could think the feasibility of renewable systems connected to grid or off-grid are similar when the economic parameters are analysed. However, the use of FPV (Configuration D or F) is more interesting from a sustainability

point of view, since they showed other sustainable advantages in terms of use of water surface and reduction of the evaporation.

The analysis of LCOE values of the hybrid systems showed the results are aligned with other published proposals, improving in many cases. Appendix 3 showed LCOE values above 0.08 €/kWh when the maximum reached LCOE value was 0.04 €/kWh in the irrigation system located in Villena, which is around 30 km from this case study and they have similar characteristics [79]. Configuration A showed is not feasible in any case. The consideration of the PAT systems according to flow over time and the demand value

caused this unfeasibility. The rest of the configuration showed feasibility in all hypotheses when the public investment is considered and all hypotheses when the energy price is increased. Configuration B showed LCOE values, which oscillated between 0.472 and 0.846 €/kWh. The lowest value was reached in the P-2 system when the discount rate was 0.04, there was no public investment and the analysis considered the current price of the energy. The highest value was reached at the value of 0.07, current price, no public investment and it was in the P-1 system.

Some of the situations analysed in Appendix 3 were chosen to develop a sensitivity analysis when economical parameters change. Fig. 12 shows this analysis when it was applied in five scenarios (one of each feasible configuration according to Appendix 3). Seven economic parameters were analysed as a function of the configuration analysed. When Configuration B has analysed its sensitivity considering the lifetime, Investment Cost of Recovery System and Annual Cost of Injected and Recovery Systems. When these parameters decreased a 25%, the LCOE value varied 1.91%, –6.55% and –14.5% respectively. If the parameter economic increased a 25%, The LCOE value changed –1.43%, 8.18% and 18.13% respectively. When Savings were analysed, this value changed –29.98%, 65.15%, and 55.08% when the economic parameters (i.e., Lifetime, Annual Cost of Injected and Recovery systems) decreased by a value of 25%. If they increased 25%, the saving value oscillated 29.03%, –81.36% and –55.08%. This variation is aligned with the variation shown by Ref. [49].

This analysis was analysed in Configuration C for the scenario, which considers a discount rate of 0.07, K equal to 0.5 and future energy prices. This configuration showed a value of 0.089€/kWh and Savings equal to 100%. The LCOE and Saving variation can be observed in Fig. 12b for the following parameters: lifetime, Investment Cost of the recovery system, Annual Cost injected and recovery systems, investment cost and the annual cost of the photovoltaic system, investment cost and annual cost of the battery. The maximum variation of the LCOE was 11.46% when the investment cost of the photovoltaic system increased a 25%. A similar trend can be observed in Fig. 12c in Configuration E.

Fig. 12c shows variations of the LCOE, which oscillated between –7.64% and 6.97% when the economic parameters increased by 25%. When these parameters decreased 25%, the LCOE values varied between –5.28% and 4.16%. Saving values changed between –13.14% and 14.09% when the parameters increased 25%, while the values oscillated between –17.61% and 9.59% when the parameters decreased 25%.

Fig. 12d shows the sensitivity analysis of configuration D, analysing the variation of the different economic parameters as lifetime, the investment cost of recovery systems, annual costs of injected and recovery systems, investment cost and the annual cost of photovoltaic systems. LCOE value varied between –9.18% and 5.25% for the different parameters increasing a 25%. LCOE value oscillated between –3.65% and 11.44% when the parameters decreased by 25%. Saving values varied between –9% and 15.44% when the parameters increased a 25% while the saving values oscillated between –19.29% and 6.03% when the parameters decreased a 25%. A similar trend showed Fig. 12e.

#### 4. Conclusions

The sustainability improvement of the different targets included in the different sustainable development goals implies the water managers must define new strategies, which define the establishment of new investments and making-decision in this alignment. In this line, this research proposes a new optimization procedure, which enables the making-decision by water managers to consider the use of photovoltaic systems and microhydropowers when their

facilities have energy consumption points (e.g., pump stations).

The research proposes a global optimization of the system, on the one hand, it considers hydraulic optimization and on the other hand, it develops the photovoltaic optimization in which the optimum capacity is related to the surface area to be occupied, considering the optimum tilt angle. The capacity of the batteries is optimized according to the existing hourly energy balances for each day of the year. The discretization was considered based on other published researches [80,81]. It enables the getting of the maximum capacity necessary to deal with the potentially accumable excess energy and periods of energy shortage.

The new proposed approach is optimized by two simulated annealing procedures, which choose the best location of the microhydropowes system and the selection of the best machine between a database of 674 pumps working as turbines. These recovery systems were defined by estimating the characteristic curves using adimensional numbers and the database of tested machines. The used objective function was the LCOE and the location definition and machine selection were developed considering the criteria of minimum service pressure to guarantee the demanded flow in each irrigation point. As a novel, the proposed methodology considered the use of the FPV or GPV analyzing different configurations to develop a deep techno-feasible analysis by an iterative procedure. It considered different farmed area scenarios, different GPV and FPV areas as well as the connection on the grid of the system or storage in batteries. This procedure considered both economic and environmental indexes to develop a feasible analysis. This proposal is a new challenge in the improvement of the self-consumption in irrigation systems since there were others published researchers, which analysed the use of PV panels in pumped stations between source and deposit or in discretized pumped irrigation systems. As a new ahead step, this research proposes the optimization using renewable energies considering both green energy systems (i.e., hydraulic and solar), which were applied in an irrigation pressurized system with both pumped and gravity distributed system considering the on-demand operation flow.

The definition of the feasible analysis showed the feasibility of the proposals for both GPV and FPV as a function of the area and discount rates, determining savings above 15% compared to current systems, which are connected to the grid to supply the pump stations. The strength of the methodology abides in its powerful to solve the different configurations using different hybrid renewable systems, which depends on the specific variables discretized and defined by the proposed optimization procedure, considering the variation of the farmed area, which influences the making-decision. LCOE values oscillated between 0.04 and 0.10 €/kWh both connected off-grid and on-grid when different configurations and scenarios such as discount rate, energy price and public investment, considering both photovoltaic and microhydropower systems. The increase in the energy price showed a decrease in the LCOE value in both operation systems, although the use of FPV systems (Configuration D) could be more interesting if the sustainable value of the decrease of the evaporation and use of the water surface are considered. The evolution of the different investments and annual costs will help to decide the selection of the best configuration. The use of hydropowers systems demonstrated it is not feasible if the PV systems are not considered (Configuration A and B), a consequence of the topology of the water system and the variability of the circulating flows in the recovery systems and the pumped station, which could not be coincided.

A robust sensitivity analysis was developed and it showed the influence of the different parameters in the variation of the LCOE and Saving values, showing a SCI above 0.93. The optimization procedure improved the different indicators values. This methodology improves the achievement of the targets included in the



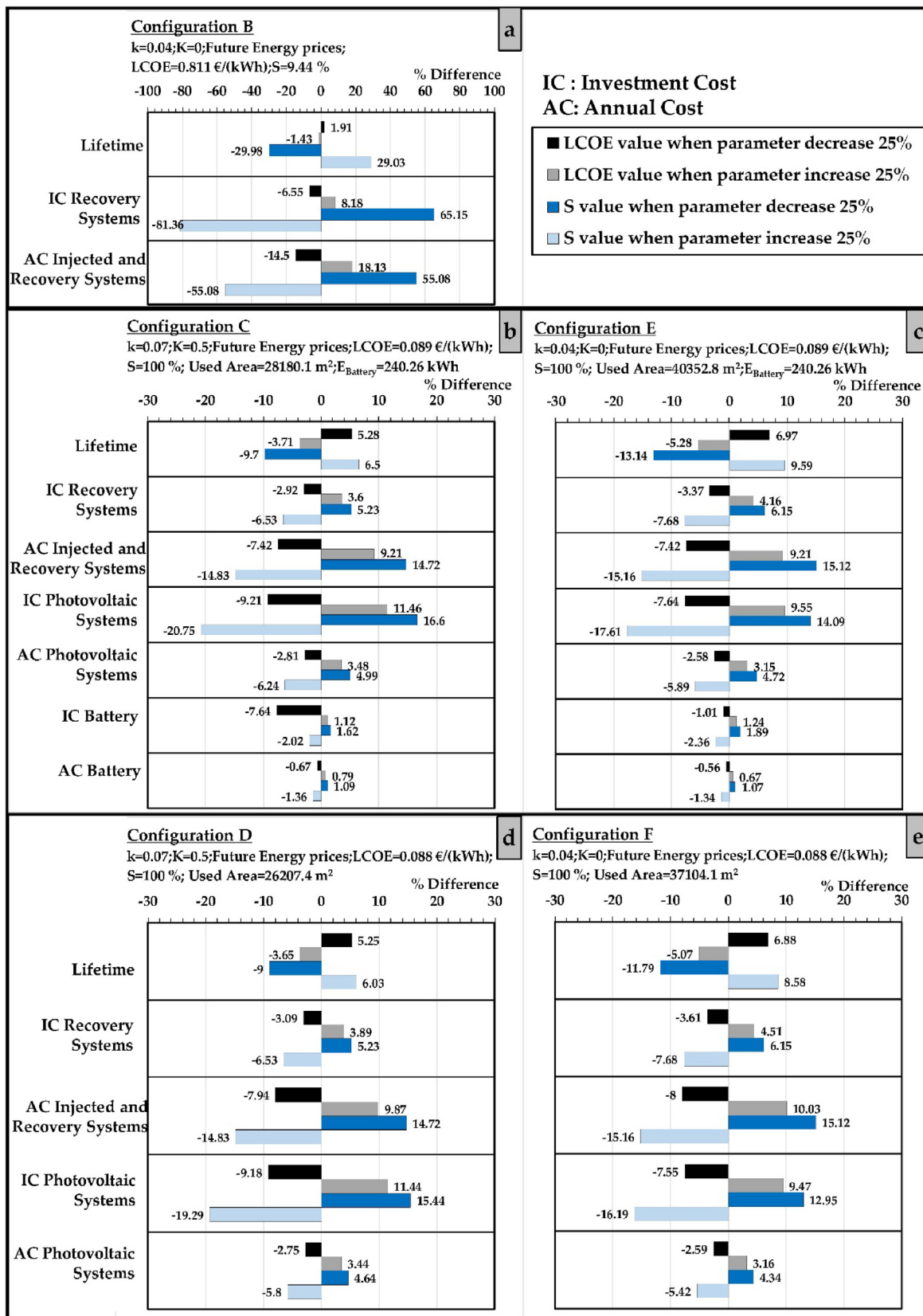


Fig. 12. Sensitivity analysis of the LCOE and Saving value for the different configurations (a) Configuration B; (b) Configuration C; (c) Configuration E; (d) Configuration D; (e) Configuration F.

sustainable development goals, particularly, the SDG-11, which is focused on sustainable cities and communities and its application, analysis and studies should be targeted by the different managers of the communities.

### Author contributions

Conceptualization, methodology and software: MPS and FJSR; validation and formal analysis: AVMG, MPS, FJSR; writing—original draft preparation, writing—review and editing, PALJ, MPS, AVMG; supervision, PALJ; final review MPS, PALJ All authors have read and agreed to the published version of the manuscript.

### Fundings

Grant PID2020-114781RA-I00 funded by MCIN/AEI/10.13039/501100011033.

### Declaration of competing interest

The authors declare that they have no known competing financial interests or personal relationships that could have appeared to influence the work reported in this paper.

### References

- [1] M.A. Pardo, J. Manzano, E. Cabrera, J. García-Serra, Energy audit of irrigation networks, *Biosyst. Eng.* 115 (2013) 89–101, <https://doi.org/10.1016/j.biosystemseng.2013.02.005>.
- [2] G. Dandy, A. Roberts, C. Hewitson, P. Chrystie, Sustainability Objectives for the Optimization of Water Distribution Networks, 8th Annu. Water Distrib. Syst. Anal. Symp. 2006, 2007, p. 83, [https://doi.org/10.1061/40941\(247\)83](https://doi.org/10.1061/40941(247)83).
- [3] I. Fernández García, A. Mc Nabola, Maximizing hydropower generation in gravity water distribution networks: determining the optimal location and number of pumps as turbines, *J. Water Resour. Plann. Manag.* 146 (2020), 04019066, [https://doi.org/10.1061/\(ASCE\)WR.1943-5452.0001152](https://doi.org/10.1061/(ASCE)WR.1943-5452.0001152).
- [4] M. Molinos-Senante, F. Hernández-Sancho, M. Mocholí-Arce, R. Sala-Garrido, A management and optimisation model for water supply planning in water deficit areas, *J. Hydrol.* 515 (2014) 139–146, <https://doi.org/10.1016/j.jhydrol.2014.04.054>.
- [5] B. Caniglia, B. Frank, B. Kerner, T.L. Mix, Water policy and governance networks: a pathway to enhance resilience toward climate change, *Socio. Forum* 31 (2016) 828–845, <https://doi.org/10.1111/sofc.12275>.
- [6] P. Saccon, Water for agriculture, irrigation management, *Appl. Soil Ecol.* 123 (2018) 793–796, <https://doi.org/10.1016/j.apsoil.2017.10.037>.
- [7] J. Benavides, E. Hernández-Plaza, L. Mateos, E. Fereres, A global analysis of irrigation scheme water supplies in relation to requirements, *Agric. Water Manag.* 243 (2021), 106457, <https://doi.org/10.1016/j.agwat.2020.106457>.
- [8] R. Cvejić, M. Pintar, V. Zupanc, Advancing irrigation development in the European union\*, *Irrig. Drain* 70 (2021) 887–899, <https://doi.org/10.1002/IRD.2585>.
- [9] J. Berbel, A. Expósito, C. Gutiérrez-Martín, L. Mateos, Effects of the irrigation modernization in Spain 2002–2015, *Water Resour. OR Manag.* 33 (2019) 1835–1849, <https://doi.org/10.1007/s11269-019-02215-W/TABLES/1>.
- [10] G.V. Lombardi, R. Berni, Renewable energy in agriculture: farmers willingness-to-pay for a photovoltaic electric farm tractor, *J. Clean. Prod.* 313 (2021), 127520, <https://doi.org/10.1016/j.jclepro.2021.127520>.
- [11] J. Mundo-Hernández, B. De Celis Alonso, J. Hernández-Álvarez, B. De Celis-Carrillo, An overview of solar photovoltaic energy in Mexico and Germany, *Renew. Sustain. Energy Rev.* 31 (2014) 639–649, <https://doi.org/10.1016/j.rser.2013.12.029>.
- [12] A.A. Ghoneim, Design optimization of photovoltaic powered water pumping systems, *Energy Convers. Manag.* 47 (2006) 1449–1463, <https://doi.org/10.1016/j.enconman.2005.08.015>.
- [13] N.S. Wahyuni, S. Wulandari, E. Wulandari, D.S. Pamuji, Integrated Communities for the Sustainability of Renewable Energy Application: Solar Water Pumping System in Banyumeneng Village, Indonesia, Elsevier B.V., 2015, <https://doi.org/10.1016/j.egypro.2015.11.604>.
- [14] A.K. Tiwari, V.R. Kalamkar, Performance investigations of solar water pumping system using helical pump under the outdoor condition of Nagpur, India, *Renew. Energy* 97 (2016) 737–745, <https://doi.org/10.1016/j.renene.2016.06.021>.
- [15] P. Periasamy, N.K. Jain, I.P. Singh, A review on development of photovoltaic water pumping system, *Renew. Sustain. Energy Rev.* 43 (2015) 918–925, <https://doi.org/10.1016/j.rser.2014.11.019>.
- [16] D.B. Singh, A. Mahajan, D. Devli, K. Bharti, S. Kandari, G. Mittal, A mini review on solar energy based pumping system for irrigation, *Mater. Today Proc.* 43 (2020) 417–425, <https://doi.org/10.1016/j.matpr.2020.11.716>.
- [17] C. Ferrer-Gisbert, J.J. Ferrán-Gozálvez, M. Redón-Santafé, P. Ferrer-Gisbert, F.J. Sánchez-Romero, J.B. Torregrosa-Soler, A new photovoltaic floating cover system for water reservoirs, *Renew. Energy* 60 (2013) 63–70, <https://doi.org/10.1016/j.renene.2013.04.007>.
- [18] R. Sharma, S. Sharma, S. Tiwari, Design optimization of solar PV water pumping system, *Mater. Today Proc.* 21 (2020) 1673–1679, <https://doi.org/10.1016/j.matpr.2019.11.322>.
- [19] P. Abhilash, R.N. Kumar, R.P. Kumar, Solar powered water pump with single axis tracking system for irrigation purpose, *Mater. Today Proc.* 39 (2020) 553–557, <https://doi.org/10.1016/j.matpr.2020.08.336>.
- [20] S. Orts-Grau, P. Gonzalez-Altozano, F.J. Gimeno-Sales, I. Balbastre-Peralta, C.I.M. Marquez, M. Gasque, S. Seguí-Chilet, Photovoltaic water pumping: comparison between direct and lithium battery solutions, *IEEE Access* 9 (2021) 101147–101163, <https://doi.org/10.1109/ACCESS.2021.3097246>.
- [21] A. Khiareddine, C. Ben Salah, M.F. Mimouni, Power management of a photovoltaic/battery pumping system in agricultural experiment station, *Sol. Energy* 112 (2015) 319–338, <https://doi.org/10.1016/j.solener.2014.11.020>.
- [22] A. Bhattacharjee, D.K. Mandal, H. Saha, Design of an Optimized Battery Energy Storage Enabled Solar PV Pump for Rural Irrigation, 1st IEEE Int. Conf. Power Electron. Intell. Control Energy Syst. ICPEICES 2016, 2017, <https://doi.org/10.1109/ICPEICES.2016.7853237>.
- [23] O. Djelailia, M.S. Kelaiaia, H. Labar, S. Necaibia, F. Merad, Energy hybridization photovoltaic/diesel generator/pump storage hydroelectric management based on online optimal fuel consumption per kWh, *Sustain. Cities Soc.* 44 (2019) 1–15, <https://doi.org/10.1016/j.scs.2018.09.037>.
- [24] T. Tezer, R. Yaman, G. Yaman, Evaluation of approaches used for optimization of stand-alone hybrid renewable energy systems, *Renew. Sustain. Energy Rev.* 73 (2017) 840–853, <https://doi.org/10.1016/j.rser.2017.01.118>.
- [25] A. Ghasemi, Coordination of pumped-storage unit and irrigation system with intermittent wind generation for intelligent energy management of an agricultural microgrid, *Energy* 142 (2018) 1–13, <https://doi.org/10.1016/j.energy.2017.09.146>.
- [26] S. Gualteros, D.R. Rousse, Solar water pumping systems: a tool to assist in sizing and optimization, *Sol. Energy* 225 (2021) 382–398, <https://doi.org/10.1016/j.solener.2021.06.053>.
- [27] D.B. Singh, A. Mahajan, D. Devli, K. Bharti, S. Kandari, G. Mittal, A mini review on solar energy based pumping system for irrigation, *Mater. Today Proc.* 43 (2021) 417–425, <https://doi.org/10.1016/j.matpr.2020.11.716>.
- [28] U. Caldera, A. Sadiqa, A. Gulagi, C. Breyer, Irrigation efficiency and renewable energy powered desalination as key components of Pakistan's water management strategy, *Smart Energy* 4 (2021), 100052, <https://doi.org/10.1016/j.segy.2021.100052>.
- [29] J. Jayaraman, T. Sudhakar, S.S. Muthukrishnan, A. Gopikanna, V. Vijayaraghavan, Irrigation Optimization for Agriculture Productivity: Case Study of a Hybrid Solar Microgrid in Rural India, 2019 IEEE Glob. Humanit. Technol. Conf. GHTC 2019, 2019, <https://doi.org/10.1109/GHTC46095.2019.9033074>.
- [30] P.E. Campana, H. Li, J. Zhang, R. Zhang, J. Liu, J. Yan, Economic optimization of photovoltaic water pumping systems for irrigation, *Energy Convers. Manag.* 95 (2015) 32–41, <https://doi.org/10.1016/j.enconman.2015.01.066>.
- [31] M.A.P. Picazo, J.M. Juárez, D. García-Márquez, Energy consumption optimization in irrigation networks supplied by a standalone direct pumping photovoltaic system, *10 (2018) 4203, Sustain. Times* 10 (2018) 4203, <https://doi.org/10.3390/SU10114203>.
- [32] M.N. Zidan, M.Y. Abdelmoez, A.N. Ahmed, R. Sobh, H. Hisham, A.A. El-Deib, Hybrid irrigation system in Egypt: design and optimization, *NILES 2021 - 3rd nov, Intell. Lead. Emerg. Sci. Conf. Proc.* (2021) 336–340, <https://doi.org/10.1109/NILES53778.2021.9600517>.
- [33] J. Carroquino, R. Dufo-López, J.L. Bernal-Aguistin, Sizing of off-grid renewable energy systems for drip irrigation in Mediterranean crops, *Renew. Energy* 76 (2015) 566–574, <https://doi.org/10.1016/j.renene.2014.11.069>.
- [34] R. Shaik, N. Beemkumar, H. Adharsha, K. Venkadeshwaran, A.D. Dhass, Efficiency enhancement in a PV operated solar pump by effective design of VFD and tracking system, *Mater. Today Proc.* 33 (2020) 454–462, <https://doi.org/10.1016/j.matpr.2020.05.035>.
- [35] A.K. Tiwari, V.R. Kalamkar, R.R. Pande, S.K. Sharma, V.C. Sontake, A. Jha, Effect of head and PV array configurations on solar water pumping system, *Mater. Today Proc.* 46 (2020) 5475–5481, <https://doi.org/10.1016/j.matpr.2020.09.200>.
- [36] M. Chahartaghi, A. Nikzad, Exergy, environmental, and performance evaluations of a solar water pump system, *Sustain. Energy Technol. Assessments* 43 (2021), 100933, <https://doi.org/10.1016/j.seta.2020.100933>.
- [37] I. Samora, M.J. Franca, A.J. Schleiss, H.M. Ramos, Simulated annealing in optimization of energy production in a water supply network, *Water Resour. Manag.* 30 (2016) 1533–1547, <https://doi.org/10.1007/s11269-016-1238-5>.
- [38] A. Morabito, P. Hendrick, Pump as turbine applied to micro energy storage and smart water grids: a case study, *Appl. Energy* 241 (2019) 567–579, <https://doi.org/10.1016/j.apenergy.2019.03.018>.
- [39] A. Carravetta, O. Fecarotta, G. Del Giudice, H. Ramos, Energy recovery in water systems by PATs: a comparisons among the different installation schemes, *Procedia Eng.* 70 (2014) 275–284, <https://doi.org/10.1016/j.proeng.2014.02.031>.
- [40] O. Fecarotta, C. Aricò, A. Carravetta, R. Martino, H. Ramos, Hydropower potential in water distribution networks: pressure control by PATs, *Water Resour. OR Manag.* 29 (2014) 699–714, <https://doi.org/10.1007/s11269-014-0836-3>.

- [41] M. Pérez-Sánchez, F.J. Sánchez-Romero, P.A. López-Jiménez, H.M. Ramos, PATs selection towards sustainability in irrigation networks: simulated annealing as a water management tool, *Renew. Energy* 116 (2018), <https://doi.org/10.1016/j.renene.2017.09.060>.
- [42] G. de Oliveira e Silva, P. Hendrick, Pumped hydro energy storage in buildings, *Appl. Energy* 179 (2016) 1242–1250, <https://doi.org/10.1016/j.apenergy.2016.07.046>.
- [43] A. Merida García, J. Gallagher, M. Crespo Chacón, A. Mc Nabola, The environmental and economic benefits of a hybrid hydropower energy recovery and solar energy system (PAT-PV), under varying energy demands in the agricultural sector, *J. Clean. Prod.* 303 (2021), 127078, <https://doi.org/10.1016/j.jclepro.2021.127078>.
- [44] R.B. Sowby, Correlation of energy management policies with lower energy use in public water systems, *J. Water Resour. Plann. Manag.* 144 (2018), 06018007, [https://doi.org/10.1061/\(asce\)wr.1943-5452.0001006](https://doi.org/10.1061/(asce)wr.1943-5452.0001006).
- [45] V. Kanakoudis, S. Tsitsifli, P. Samaras, A. Zouboulis, G. Demetriou, Developing appropriate performance indicators for urban distribution systems evaluation at Mediterranean countries, *Water Util. J.* (2011) 31–40.
- [46] P. Duarte, D.I.C. Covas, H. Alegre, PI for assessing effectiveness of energy management processes in water supply systems, *IWA Int. Conf. PI09* (2009).
- [47] L.A. Rossman, The EPANET Programmer's Toolkit for Analysis of Water Distribution Systems, WRPMD 1999 Prep. 21st Century, 1999, pp. 1–10, [https://doi.org/10.1061/40430\(1999\)39](https://doi.org/10.1061/40430(1999)39).
- [48] M. Pérez-Sánchez, F. Sánchez-Romero, H. Ramos, P. López-Jiménez, Modeling irrigation networks for the quantification of potential energy recovering: a case study, *Water* 8 (2016) 1–26, <https://doi.org/10.3390/w8060234>.
- [49] S. Abdelhady, Performance and cost evaluation of solar dish power plant: sensitivity analysis of leveled cost of electricity (LCOE) and net present value (NPV), *Renew. Energy* 168 (2021) 332–342, <https://doi.org/10.1016/j.renene.2020.12.074>.
- [50] A. Al-Karaghoul, L.L. Kazmerski, Optimization and life-cycle cost of health clinic PV system for a rural area in southern Iraq using HOMER software, *Sol. Energy* 84 (2010) 710–714, <https://doi.org/10.1016/j.solener.2010.01.024>.
- [51] C.A.M. Avila, F.-J. Sánchez-Romero, P.A. López-Jiménez, M. Pérez-Sánchez, Definition of the operational curves by modification of the affinity laws to improve the simulation of PATs, *Water* 13 (2021) 1880, <https://doi.org/10.3390/w13141880>, 13 (2021) 1880.
- [52] J. Baptista, P. Vargas, J. Baptista, P. Vargas, J.R. Ferreira, ICREPQ'21 Almería (Spain), 28 th to 30 th, *Renew. Energy Power Qual. J.* (2021), <https://doi.org/10.24084/repqj19.214>.
- [53] M. Redón Santafé, J.B. Torregrosa Soler, F.J. Sánchez Romero, P.S. Ferrer Gisbert, J.J. Ferrán Gozávez, C.M. Ferrer Gisbert, Theoretical and experimental analysis of a floating photovoltaic cover for water irrigation reservoirs, *Energy* 67 (2014) 246–255, <https://doi.org/10.1016/j.energy.2014.01.083>.
- [54] A. Sahu, N. Yadav, K. Sudhakar, Floating photovoltaic power plant: a review, *Renew. Sustain. Energy Rev.* 66 (2016) 815–824, <https://doi.org/10.1016/j.rser.2016.08.051>.
- [55] I.F. García, D. Novara, A. Mc Nabola, A model for selecting the most cost-effective pressure control device for more sustainable water supply networks, *Water* 11 (2019) 1297, <https://doi.org/10.3390/w11061297>.
- [56] C. Bousquet, I. Samora, P. Manso, L. Rossi, P. Heller, A.J. Schleiss, Assessment of hydropower potential in wastewater systems and application to Switzerland, *Renew. Energy* 113 (2017) 64–73, <https://doi.org/10.1016/j.renene.2017.05.062>.
- [57] A. Carravetta, G. Del Giudice, O. Fecarotta, H. Ramos, PAT design strategy for energy recovery in water distribution networks by electrical regulation, *Energies* 6 (2013) 411–424, <https://doi.org/10.3390/en6010411>.
- [58] GrupoTragsa, *Civil Works Tariffs TRAGSA 2021*, 2021.
- [59] I. Pvp's, *Trends in Photovoltaic Applications 2019, 2020*.
- [60] M. Redón Santafé, J.B. Torregrosa Soler, F.J. Sánchez Romero, P.S. Ferrer Gisbert, J.J. Ferrán Gozávez, C.M. Ferrer Gisbert, Theoretical and experimental analysis of a floating photovoltaic cover for water irrigation reservoirs, *Energy* 67 (2014) 246–255, <https://doi.org/10.1016/j.energy.2014.01.083>.
- [61] U.S.E.I. Administration, *U.S. Average Installed Utility-Scales Battery Storage Cost(2015-2018)*, 2021.
- [62] C. González-Pavón, J. Arviza-Valverde, I. Balbastre-Peralta, J.M.C. Sierra, G. Palau-Salvador, Are water user associations prepared for a second-generation modernization? The case of the Valencian community (Spain), *Water* 12 (2020) 2136, <https://doi.org/10.3390/w12082136>.
- [63] L. Micheli, Energy and economic assessment of floating photovoltaics in Spanish reservoirs: cost competitiveness and the role of temperature, *Sol. Energy* 227 (2021) 625–634, <https://doi.org/10.1016/j.solener.2021.08.058>.
- [64] C. Giudicianni, M. Herrera, A. di Nardo, A. Carravetta, H.M. Ramos, K. Adeyeye, Zero-net energy management for the monitoring and control of dynamically-partitioned smart water systems, *J. Clean. Prod.* 252 (2020), 119745, <https://doi.org/10.1016/j.jclepro.2019.119745>.
- [65] D.L. Talavera, E. Muñoz-Cerón, J.P. Ferrer-Rodríguez, P.J. Pérez-Higueras, Assessment of cost-competitiveness and profitability of fixed and tracking photovoltaic systems: the case of five specific sites, *Renew. Energy* 134 (2019) 902–913, <https://doi.org/10.1016/j.renene.2018.11.091>.
- [66] M. Khastar, A. Aslani, M. Nejati, How does carbon tax affect social welfare and emission reduction in Finland? *Energy Rep.* 6 (2020) 736–744, <https://doi.org/10.1016/j.egyr.2020.03.001>.
- [67] S. Rausch, H. Yonezawa, The intergenerational incidence of green tax reform, *Clim. Chang. Econ.* 9 (2018), 1840007, <https://doi.org/10.1142/S2010007818400079>.
- [68] L. Romero, M. Pérez-Sánchez, P.A. López-jiménez, Water implications in Mediterranean irrigation networks: problems and solutions, *Int. J. Energy Environ.* 8 (2017) 8396, [http://ijee.ieefoundation.org/vol2/public\\_html/ijeeindex/vol2/issue4/IJEE\\_03\\_v2n4.pdf](http://ijee.ieefoundation.org/vol2/public_html/ijeeindex/vol2/issue4/IJEE_03_v2n4.pdf).
- [69] E. and T.M. Spanish Government, Factores de emisión de CO2 y coeficientes de paso a energía primaria de diferentes fuentes de energía final consumidas en el sector de edificios en España, 2016 [PDF][647,80 KB], [https://energia.gob.es/desarrollo/EficienciaEnergetica/RITE/Reconocidos/Reconocidos/Otros documentos/Factores\\_emision\\_CO2.pdf](https://energia.gob.es/desarrollo/EficienciaEnergetica/RITE/Reconocidos/Reconocidos/Otros documentos/Factores_emision_CO2.pdf). (Accessed 27 March 2022).
- [70] F.V. Marcos, F.V. Marcos, Á. de la C. Mera, M. del R.H. Celemin, Vivienda y salud: eficiencia energética, urbanismo sostenible y agenda 2030, Conclusiones y futuro, *Rev. Salud Ambient.* 21 (2021) 56–64, <https://ojs.diffundit.com/index.php/rsa/article/view/1102>. (Accessed 13 November 2021).
- [71] BOE, BOE-A-2021-4572 Real Decreto 178/2021, de 23 de marzo, por el que se modifica el Real Decreto 1027/2007, de 20 de julio, por el que se aprueba el Reglamento de Instalaciones Térmicas en los Edificios, 2021. <https://www.boe.es/buscar/doc.php?id=BOE-A-2021-4572>. (Accessed 13 November 2021).
- [72] S. Rausch, H. Yonezawa, THE INTERGENERATIONAL INCIDENCE OF GREEN TAX REFORM, <https://doi.org/10.1142/S2010007818400079>, 9, 2018, 1840007, <https://doi.org/10.1142/S2010007818400079>.
- [73] M. Mitscher, R. Rüther, Economic performance and policies for grid-connected residential solar photovoltaic systems in Brazil, *Energy Pol.* 49 (2012) 688–694, <https://doi.org/10.1016/j.enpol.2012.07.009>.
- [74] M. Pérez-Sánchez, F.J. Sánchez-Romero, P.A. López-Jiménez, Nexo agua-energía: optimización energética en sistemas de distribución. Aplicación 'Postrasvase Júcar-Vinalopó,' *Tecnol. y Ciencias Del Agua* 8 (2017) 19–36, <https://doi.org/10.24850/j-TYCA-2017-04-02>.
- [75] M. Pérez-Sánchez, F.J. Sánchez-Romero, H.M. Ramos, P.A. López-Jiménez, Calibrating a flow model in an irrigation network: case study in Alicante, Spain, *Spanish J. Agric. Res.* 15 (2017), e1202, <https://doi.org/10.5424/sjar/2017151-10144>.
- [76] SIAR, Siar, (n.d.). <https://eportal.mapa.gob.es/websiar/Inicio.aspx> (accessed October 12, 2021).
- [77] F.J. Lugauer, J. Kainz, M. Gaderer, Techno-economic efficiency analysis of various operating strategies for micro-hydro storage using a pump as a turbine, *Energies* 14 (2021), <https://doi.org/10.3390/en14020425>.
- [78] E. Vartiainen, G. Masson, C. Breyer, PV LCOE in Europe 2014-30 - Final Report, 23 June 2015, 2015. *Eur. PV Technolgy Platf. Steer. Comm. PV LCOE Work. Gr.* [http://www.etip-pv.eu/fileadmin/Documents/FactSheets/English2015/PV\\_LCOE\\_Report\\_July\\_2015.pdf](http://www.etip-pv.eu/fileadmin/Documents/FactSheets/English2015/PV_LCOE_Report_July_2015.pdf).
- [79] I.B. Carrêlo, R.H. Almeida, L. Narvarte, F. Martínez-Moreno, L.M. Carrasco, Comparative analysis of the economic feasibility of five large-power photovoltaic irrigation systems in the Mediterranean region, *Renew. Energy* 145 (2020) 2671–2682, <https://doi.org/10.1016/j.renene.2019.08.030>.
- [80] V.A. Ani, Feasibility and optimal design of a stand-alone photovoltaic energy system for the orphanage, 2014, *J. Renew. Energy.* (2014) 1–8, <https://doi.org/10.1155/2014/379729>.
- [81] B.A. Aderemi, S.P. Daniel Chowdhury, T.O. Olwal, A.M. Abu-Mahfouz, Techno-economic feasibility of hybrid solar photovoltaic and battery energy storage power system for a mobile cellular base station in soshanguve, South Africa, *Energies* 11 (2018) 1572, <https://doi.org/10.3390/EN11061572>.